IgM$^+$ and IgG$^+$ memory B cells represent heterogeneous populations capable of producing class-switched antibodies and germinal center B cells upon re-challenge with *P. yoelii*.

Susie L. Brown[1], Jonathan J. Bauer-Erickson[1], Juhyung Lee[1], Enatha Ntirandekura[1], and Jason S. Stumhofer[1].

[1]Department of Microbiology and Immunology, University of Arkansas for Medical Sciences, Little Rock, AR, USA.

Correspondence should be addressed to J.S.S. (jstumhofer@uams.edu), University of Arkansas for Medical Sciences, Department of Microbiology and Immunology, Room 521A, 4301 W. Markham St., Little Rock, AR. Phone no. – 501-526-6180.

Abstract

Memory B cells (MBCs) are essential for maintaining long-term humoral immunity to infectious organisms, including *Plasmodium*. MBCs are a heterogeneous population whose function can be dictated by isotype or expression of particular surface proteins. Here, aided by the use of antigen-specific B cell tetramers, MBC populations were evaluated to discern their phenotype and function in response to infection with a non-lethal strain of *P. yoelii*. Infection of mice with *P. yoelii* 17X resulted in the production of three predominant MBC populations: somatically hypermutated isotype-switched (swIg$^+$) and IgM$^+$ MBCs that co-expressed CD73 and CD80, and CD73$^-$CD80$^-$ unmutated swIg$^+$ B cells. Re-challenge experiments indicated that IgG-producing cells dominated the recall response with minimal induction of IgM-secreting cells. Furthermore, using fluorescent protein expression as a surrogate for CD73 and CD80 co-expression, ZsGreen1$^+$IgM$^+$ MBCs gave rise to class switched IgG-producing plasmablasts that induced comparable titers of Ag-specific Abs as their swIg$^+$ counterparts after adoptive transfer and *P. yoelii* infection. Moreover, ZsGreen1$^+$ IgM$^+$ and swIg$^+$ MBCs gave rise to B cells with a germinal center phenotype. Together these data indicated that MBC function is not defined by immunoglobulin isotype, nor does co-expression of key surface markers limit the potential fate of MBCs after recall.

Introduction

Memory B cells (MBCs) represent a population of B cells that serve to protect the host upon antigen (Ag) re-encounter. They can differentiate into antibody-secreting cells (ASCs) upon Ag recognition,[1] and there is additional evidence that indicates that MBCs possess the ability to re-enter the germinal center (GC) for further rounds of somatic hypermutation.[2–4] While MBCs play an essential role in infection- and vaccine-induced protective immunity, many aspects of their generation, maintenance, and function in secondary responses remain vague. However, recent findings have shed new light on the biology of this cell type. Once thought of as a homogeneous cell population that expresses class-switched, somatically hypermutated B cell receptors (BCRs) generated within a GC, MBCs are instead a diverse heterogenic population of cells with a GC-dependent and -independent origin.[5,6] Nevertheless, interpreting these recent findings on the biology of MBCs has proved to be complex. For instance, the ability of MBCs to re-enter the GC remains a point of controversy,[7–9] as this event may be restricted to IgM^+ MBCs and depend on the presence of persistent GCs.[3,10] Also, recent evidence indicates that a bottleneck event occurs that restricts the ability of MBCs to re-enter the GC.[11] Conversely, others suggest that isotype-switched MBCs can re-enter GCs after challenge.[12] In contrast, other evidence indicates that functionality is defined based on the presence or absence of cell surface markers, such as CD80, PD-L2, and CD73, rather than the isotype of the BCR.[2,13,14] These findings suggest functional heterogenicity within the MBC pool. However, the contradicting results are likely the product of the models utilized to evaluate MBC function and highlight the need for additional studies to assess MBC heterogeneity on functional outcome, particularly in the context of infection-induced responses.

Studies in humans link *Plasmodium*-specific antibody (Ab) responses to protection from clinical disease.[15–19] Additionally, experimental mouse models of malaria indicate that B cells and Abs are required for clearance of primary infections and protection against re-infection.[20–24] Generation of long-lived plasma cells and MBCs during primary infection and their subsequent maintenance are needed for protection from secondary infections. However, the acquisition of Ab-mediated immunity against *Plasmodium* varies based on the number of exposures during each transmission season.[25,26] Although there is evidence in humans that MBCs and parasite-specific Abs can be maintained for long periods after infection,[27–32] there is also evidence that a portion of MBCs generated against malarial antigens appear to be short-lived, and parasite-specific Ab titers drop rapidly with low re-infection rates.[33–37] A similar drop in parasite-specific MBCs also occurs in mice over time after *P. chabaudi* infection.[38,39] These findings highlight many of the obstacles to developing an effective malaria vaccine.

MBCs are generated after *Plasmodium* infection in mice and humans; however, knowledge of their specificity, phenotype, origin, and affinity for malarial Ags is limited, although recent reports have provided novel insights into this subset of cells. For instance, MBCs produced after primary infection give rise to a faster secondary Ab response upon re-infection with *P. chabaudi*.[38–40] A response that is initially dominated by the activation of IgM^+ MBCs and is partially dependent on $CD4^+$ T cells.[40] Here, utilizing a *P. yoelii* infection model and B cell tetramers specific for two blood-stage Ags (MSP-1_{42} and AMA-1), we sought to evaluate the formation and diversity of the MBC compartment and determine which subpopulations of MBCs respond upon re-exposure to Ag. We found that two dominant populations of MBCs emerge after infection within the IgM^+ and isotype-switched ($swIg^+$) MBC pools, those that co-expressed CD80 and CD73 and those that expressed neither of these cell surface markers. IgM^+ and $swIg^+$

MBCs that co-express CD80 and CD73 possess somatically hypermutated BCRs while the BCRs of the swIg^{+}CD80^{-}CD73^{-} MBCs contain few to no mutations, indicating a more germline state.

Expansion in MSP-1–specific B cell numbers occurred in response to re-challenge with IgG production dominant over IgM. Furthermore, using a fluorescent ZsGreen1 protein as a surrogate for CD80^{+}CD73^{+} co-expression, adoptive transfer of ZsGreen1^{+} IgM^{+} or swIg^{+} MBCs into naïve mice followed by infection with *P. yoelii* indicated that both of these MBC populations possessed the ability to differentiate into plasmablasts and eventually GC B cells. In contrast, ZsGreen1^{-} swIg^{+} B cells responded poorly to reactivation in vitro compared to their ZsGreen1^{+} counterparts. Collectively, these studies indicate that somatically hypermutated *P. yoelii*-specific CD80^{+}CD73^{+} IgM^{+} and swIg^{+} MBCs respond to reactivation through cellular expansion and differentiation into IgG-producing plasmablasts and GC B cells.

Results

MBCs segregate into heterogeneous populations based on phenotype after *P. yoelii* infection

To phenotypically define MBC subsets after infection, C57BL/6 wild-type (WT) mice were infected with a non-lethal strain (17X) of *P. yoelii*. Periodically over the course of the infection and after clearance (Supplemental Fig. 1A), spleens were harvested and stained for several phenotypic markers associated with MBCs,[13,14,41,42] including proteins that regulate T cell activity (CD80, PD-L2), enzymes involved in the generation of adenosine from ATP (CD73, CD39), the chemokine receptor CCR6, and the receptor for leukemia inhibitory factor (LIFR). While the specific role of these proteins on MBC function is largely unknown, a loss of these proteins through germline deletion or inhibition of ligand-receptor interactions can negatively impact the immune system.[43–50]

As several effector B cell populations emerge after infection, we utilized a gating strategy throughout to distinguish between $CD138^{+}CD38^{lo/-}$ plasmablasts (PBs), $CD38^{-}GL\text{-}7^{+}$ germinal center (GC) B cells, $CD38^{+}GL\text{-}7^{+}$ multipotent precursors,[5] and expanding $CD38^{+}GL\text{-}7^{-}$ MBCs in the spleen. The $CD38^{+}GL\text{-}7^{+}$ multipotent precursors represent a transitional stage in B cell differentiation that precedes the formation of GC B cells and MBCs and possesses the ability to differentiate into these populations.[5] Within the $CD138^{-}CD38^{+}GL\text{-}7^{-}$ population B cells were further subdivided into IgM^{+} and IgM^{-} ($swIg^{+}$) groups (Supplemental Figure 1B). Subsequent analysis of the MBC associated markers CD73 and CD80 revealed the segregation of IgM^{+} and $swIg^{+}$ MBCs into two predominant populations: $CD73^{+}CD80^{+}$ and $CD73^{-}CD80^{-}$ (Fig. 1A). This CD73 and CD80 expression pattern resembled that seen for nitrophenyl (NP)-specific memory B cells after immunization with NP-chicken γ-globulin (NP-CGG)[14] or infection with *P.*

chabaudi.[40] Shortly after infection, expansion in the IgM$^+$CD73$^+$CD80$^+$ population occurred, followed by a decline. Then a second expansion that peaked at day 70 post-infection (p.i.) was observed. Similarly, swIg$^+$ CD73$^+$CD80$^+$ MBC numbers peaked at day 70. While swIg$^+$CD73$^+$CD80$^+$ MBC numbers declined after day 70, the IgM$^+$CD73$^+$CD80$^+$ MBCs were steadily maintained through day 350 p.i. (Fig. 1B). However, the decline in swIg$^+$CD73$^+$CD80$^+$ MBC numbers was not as steep as that seen for the swIg$^+$CD73$^-$CD80$^-$ MBCs, which saw a >30-fold reduction in numbers from day 70 to day 350. Though the overall number of swIg$^+$CD73$^-$CD80$^-$ MBCs was higher in the spleen almost a year after infection than the swIg$^+$CD73$^+$CD80$^+$ MBCs (Fig. 1B). As the IgM$^+$CD73$^-$CD80$^-$ population encompasses MBCs and naïve B cells, it is not surprising that their numbers remained steady past day 70 p.i.

Using the expression of CD80 and CD73 to define MBC populations, the expression of the other aforementioned markers associated with MBCs was examined. The majority of the CD73$^-$CD80$^-$ cells, regardless of their isotype, did not express PD-L2. Also, PD-L2 expression was not uniform amongst the CD73$^+$CD80$^+$ cells; however, a higher frequency of swIg$^+$CD73$^+$CD80$^+$ MBCs expressed PD-L2 compared to IgM$^+$CD73$^+$CD80$^+$ MBCs (Fig. 1C). Since CD39 assists CD73 in the breakdown of ATP to adenosine,[51] it was not surprising to see that most CD73 expressing MBCs (IgM$^+$ and swIg$^+$) co-expressed CD39. Also, a high frequency (>50%) of the CD73$^-$ MBCs (IgM$^+$ and swIg$^+$) expressed CD39 (Fig. 1D). The expression of the chemokine receptor CCR6 is associated with MBC precursors found within the light zone of the GC,[52] and CD38$^+$GL-7$^+$ multipotent precursors express CCR6 as well.[5] Early on, after the infection, the per-cell expression of CCR6 was the highest for the CD38$^+$GL-7$^+$ multipotent precursors (Fig. 1E). As the infection progressed, the fluorescent intensity of CCR6 decreased on this population, correlating with the decline in this population (data not shown). Within the MBC pool, a small

proportion of IgM$^+$ and swIg$^+$ MBCs showed expression of CCR6. Still, most CD73$^+$ MBCs do not express this chemokine receptor, possibly suggesting that MBCs lose expression of this receptor with maturation or only a subset of them express it (Fig. 1E,F). Similarly, the expression of CCR6 was low amongst GC B cells upon their initial appearance but increased slightly over time (Fig. 1E). Signaling through the LIFR is linked to the self-renewal and survival of murine hematopoietic stem cells,[48,53] and it is upregulated and responsive to LIF stimulation on MBCs.[41] Here, a sizable proportion of IgM$^+$ and swIg$^+$ CD73$^+$CD80$^+$ MBCs express the LIFR while very few CD73$^-$CD80$^-$ MBCs express this receptor after *P. yoelii* infection (Fig. 1G).

Expression of CD73 by B cells is thought to be associated with the expression of activation-induced cytidine deaminase (AID) through either a GC-dependent or -independent manner, as the majority of CD73$^+$ MBCs have a high rate of somatic mutations in their BCR.[5,13,54] To confirm that CD73 and CD80 co-expression coincides with AID expression, we crossed a mouse in which cre recombinase (*aicda*$^{cre/+}$) replaces the endogenous AID protein with a mouse expressing the *R26*^{ZsGreen1} allele (Ai6). Thus, cre-mediated recombination in the subsequent offspring leads to permanent ZsGreen1 fluorescent protein marking upon expression of the *Aicda* locus (*aicda*^{cre}Ai6 mice).[55,56] Regardless of isotype, most of the CD73$^+$CD80$^+$ MBCs expressed the ZsGreen1 protein, indicating they turned on AID transcription, whereas only a small fraction of IgM$^+$ or swIg$^+$ CD73$^-$CD80$^-$ MBCs expressed ZsGreen1 (Fig. 2). Thus, CD73 and CD80 co-expression did largely correlate with AID expression.

Another layer of diversity in MBCs was recently described in the mouse model of *P. chabaudi* infection. A proportion of the IgM$^+$ MBCs also expresses high amounts of IgD on their surface.[40] Further phenotypic analysis of the IgM$^+$CD73$^-$CD80$^-$ B cells indicated that most were positive for IgD expression, suggesting that these cells are predominantly naïve B cells.

Similarly, the majority of the swIg^{+}CD73^{-}CD80^{-} B cells expressed IgD (Supplemental Fig. 1C). Since many of the swIg^{+}CD73^{-}CD80^{-} B cells do not express AID (based on the lack of ZsGreen1 fluorescence) and are IgM$^{lo/-}$, these cells may represent naïve B cells or B cells in the early stages of activation prior to class-switch recombination rather than an actual MBC population. In addition, a sizable proportion of the IgM^{+}CD73^{+}CD80^{+} B cells and a small proportion of the swIg^{+}CD73^{+}CD80^{+} were IgD^{hi} (Supplemental Fig. 1C). In all cases, the frequency of IgD^{hi} B cells within each population varied between mice.

Together these data indicate that based on differences in the expression of several cell surface proteins, MBCs represent a population of cells, at least phenotypically, with multiple layers of diversity. However, the layers of diversity seem less dependent on the isotype of the BCR but rather dependent on the experiences of the B cell itself within the environment that forms after *P. yoelii* infection, as similar phenotypic populations are present in IgM^{+} and swIg^{+} MBC pools.

Distinct MSP-1–specific plasmablasts, GC B cells, and MBCs are identifiable with a B-cell tetramer after infection.

To substantiate our findings on MBCs from examining the polyclonal B cell response after infection, we utilized a B cell tetramer to examine Ag-specific B cells. Here, a phycoerythrin (PE)-conjugated B cell tetramer consisting of the 42 kD C-terminal end of the merozoite surface protein-1 (MSP-1) from *P. yoelii* was generated. This reagent was subsequently used to label Ag-specific B cells ex vivo, followed by magnetic bead-based enrichment of the labeled cells. As components of the tetramer itself, such as PE, can be bound by B cells, splenocytes were first stained with a decoy reagent to exclude them before incubation with the MSP-1 PE tetramer.[57] Anti-PE-specific microbeads were then used to enrich the tetramer and decoy specific B cells,

which were subsequently labeled with Abs for analysis and quantitation by flow cytometry. After excluding dead cells, doublets, and non-B cells, B cell populations were identified and gated based on B220 and CD138 expression. Within this population, decoy$^-$ MSP-1$^+$ B cells were identifiable before and after *P. yoelii* infection (Fig. 3A). Tracking of MSP-1–specific B cells over one year after infection indicated that MSP-1–specific B cells rapidly expanded and peaked in cell numbers in the spleen shortly after infection and subsequently contracted by day 35. Thereafter a second but smaller expansion in cell numbers occurred and peaked by day 70 p.i. before contracting again by 100 days p.i. Hereafter the MSP-1–specific B cell numbers remained consistent over one-year p.i., but the numbers were higher than those seen in naïve mice (Fig. 3B).

To corroborate our results with the MSP-1 tetramer, a similar set of experiments was performed using a B cell tetramer composed of another blood-stage Ag, apical merozoite antigen-1 (AMA-1) (Supplemental Fig. 2A,B). Rather than peaking at day 7 p.i. as the MSP-1$^+$ B cells, AMA-1–specific B cells continued to expand in number throughout the infection, reaching their peak at day 28. Following a contraction phase, a second smaller wave of expansion occurred at day 70 before slowly contracting over time, a pattern that resembled that for the MSP-1$^+$ B cells.

MSP-1–specific B cells possessed a naïve phenotype (CD38$^+$GL-7$^-$IgM$^+$IgD$^+$) in uninfected mice (Fig. 3C, *data not shown*), while distinct populations of effector B cells were noted in the spleen after infection, including plasmablasts, MBCs, and GC B cells (Fig. 3C). Also, MSP-1–specific CD38$^+$GL-7$^+$ precursor B cells[5] were observed at days 7 and 12 after infection but were not maintained beyond this time (Fig.3C, *data not shown*). MSP-1–specific plasmablasts peaked in cell numbers by day 7 p.i. and contracted quickly by day 12 p.i. (Fig. 3D). Whereas a distinct

second wave of plasmablast formation started at 100 days after *P. chabaudi* infection and was visible out to 265 days p.i.,[40] this degree of expansion was not apparent after *P. yoelii* infection (Fig. 3C, D). MSP-1–specific GC B cells peaked at day 28 p.i. and were still detectable at 100 days p.i., but by day 168, these cells were no longer prevalent. $CD38^{+}GL\text{-}7^{-}$ B cell numbers expanded at day 7 p.i. but contracted at day 12. Then this population went through another small expansion and contraction between day 28 and 35 p.i. before a large expansion took place after this time resulting in peak numbers by day 70 p.i. Afterward, this population contracted before leveling out by 24 weeks p.i. (Fig. 3C, D). The observed gains in cell numbers most likely represent MBC production waves, GC-independent at day 7 and GC-dependent through day 70 p.i., rather than an influx of naïve B cells.

Tetramer-specific MBCs display a similar heterogenic phenotype as polyclonal MBCs

To determine if the MSP-1–specific MBCs phenotypically resembled the overall polyclonal MBC population, non-switched and switched $tetramer^{+}$ MBCs were examined for expression of CD73 and CD80 throughout infection. Similar to findings in Figure 1, MSP-1–specific IgM^{+} and $swIg^{+}$ MBCs segregated into two predominant populations: $CD73^{+}CD80^{+}$ and $CD73^{-}CD80^{-}$ over time (Fig. 4A). Very few MSP-1–specific IgM^{+} and $swIg^{+}$ cells upregulated CD73 by day 7 p.i., instead most of these $CD38^{+}GL\text{-}7^{-}$ B cells were predominantly $CD73^{-}CD80^{-}$ or $CD80^{+}$ (Fig. 4B-C, *data not shown*). Following an initial expansion and contraction in cell numbers, MSP-1–specific IgM^{+} and $swIg^{+}$ $CD73^{+}CD80^{+}$ and $CD73^{-}CD80^{-}$ MBCs peaked at day 70, after that contracting over time (Fig. 4B). Except for the MSP-1–specific $swIg^{+}$ $CD73^{+}CD80^{+}$ MBCs, which were still declining, all other populations of MSP-1–specific MBCs had stabilized by one-

year p.i. (Fig.4B,C). This pattern of MSP-1–specific MBC expansion and contraction was in line with that observed for the overall MBC population after infection (Fig. 1).

Examination of AMA-1–specific MBCs revealed some differences compared to the MSP-1–specific MBCs. While the pattern of expansion and contraction of the $CD73^{+}CD80^{+}$ MBCs looked similar, the frequency and number of AMA-1–specific IgM^{+} and $swIg^{+}$ $CD73^{-}$ $CD80^{-}$ MBCs were lower than those observed for the MSP-1–specific cells, and their cell numbers were still declining a year after the infection had cleared (Supplemental Fig. 2C-E). Overall, examining the polyclonal and Ag-specific MBC response after *P. yoelii* infection revealed that the spleen continues to generate IgM^{+} and $swIg^{+}$ MBCs well after clearance of the infection. While $CD73^{+}CD80^{+}$ IgM^{+} MBC numbers reach a point of stability after infection, there is slow attrition in $CD73^{+}CD80^{+}$ $swIg^{+}$ MBC numbers over time.

Lastly, the examination of the MSP-1–specific MBCs after *P. yoelii* infection indicated that all of the $CD73^{-}CD80^{-}$ MBCs, regardless if they were IgM^{+} or $swIg^{+}$, expressed IgD with the vast majority staining as IgD^{hi}. Approximately half of the IgM^{+} $CD73^{+}CD80^{+}$ MBCs were IgD^{hi} while the other half was $IgD^{lo/-}$. In contrast the $swIg^{+}$ $CD73^{+}CD80^{+}$ MBCs were primarily $IgD^{lo/-}$ (Supplemental Fig. 3). Hence, phenotypically distinct populations of MBCs exist in the spleen after infection with *P. yoelii*, and they resemble the populations generated in other mouse models of infection and immunization.

***Plasmodium*-specific MBC subsets are genetically distinct**

As B cells progress through the GC reaction, they accumulate mutations within their BCR, some of which increase their overall affinity for binding Ag. These high-affinity B cells can outcompete their brethren for T-cell help to maintain their survival; thus, allowing them to

undergo further rounds of replication and somatic mutation or differentiate into long-lived MBCs and plasma cells. To explore the degree of somatic mutations in the BCR of various MBC populations after clearance of *P. yoelii* infection, individual heavy and light-chains of MSP-1–specific B cells (IgM^+ and $swIg^+$ $ZsGreen1^+$, $swIg^+$ $ZsGreen1^-$) were sequenced from *aicda*^{cre}Ai6 reporter mice. As shown in figure 4D-E, the majority of the $swIg^+$ $ZsGreen1^-$ B cells displayed no mutations within their heavy and light chain genes. Furthermore, although these cells did not express IgM on their surface, they contained IgM transcripts. This finding supports the idea that these B cells are primarily naïve, immature, or recently activated and have downregulated IgM on their surface, but they have yet to undergo class-switch recombination or somatic hypermutation, hence the lack of ZsGreen1 expression. The $ZsGreen1^+swIg^+$ MSP-1–specific MBCs accumulated a significant number of somatic mutations within their V_H and V_L chains (Fig. 4D,E). Examination of their heavy chain constant region indicated that the majority of these MBCs express IgG2c, but a high frequency also expressed IgG1 or IgG2b. $IgG3^+$ clones composed the smallest fraction of the $ZsGreen1^+swIg^+$ clones sampled (Fig. 4F). While most of the $ZsGreen1^+IgM^+$ MBCs accumulated somatic mutations in their V_H or V_L chain genes, the number of mutations seen was significantly lower than the $ZsGreen1^+swIg^+$ MSP-1–specific MBCs (Fig. 4E,F).

MSP-1–specific MBCs rapidly expand after secondary infection

A hallmark of MBCs is their ability to differentiate into ASCs upon re-encounter with Ag. To determine how MBCs function during secondary infection, mice infected 90 days prior were re-challenged, i.p. with 10^6 *P. yoelii* 17X pRBCs. MSP-1_{42} tetramer$^+$ B cells were examined on the day of re-challenge and 3, 5, and 9 days after re-infection (Fig. 5A). Expansion in the number of

MSP-1_{42}^{+} B cells in the spleen occurred three days after re-challenge, and the numbers continued to rise over the next 6 days compared to the non-challenged mice (Fig. 5B). The early expansion in Ag-specific B cells after re-challenge was primarily attributed to plasmablasts. Their numbers expanded significantly over the first nine days after re-infection (Fig. 5A,C). The MSP-1_{42}^{+} $CD38^{+}GL\text{-}7^{-}$ B cells, encompassing naïve and MBCs, and the MSP-1_{42}^{+} GC B cells also saw significant expansion by days 5 and 9 p.c. respectfully (Fig. 5C).

There was little to no change in MSP-1_{42}–specific IgM titers in the serum and ASCs in the spleen after re-challenge, unlike primary infected mice, which showed a significant expansion in MSP-1_{42}–specific IgM-secreting cells at day 9 (Fig. 5D,E). In contrast, the MSP-1_{42}–specific IgG titers and ASCs in the spleen showed significant enhancement by day 5 p.c., and they remained elevated at day 9 (Fig. 5D,E). Moreover, MSP-1–specific ASCs were not detectable in the spleen of mice with a primary *P. yoelii* infection until day 9 p.i. Their numbers were significantly lower than those observed in the re-challenged mice, indicating that the MBC response dominates the humoral response during secondary infection with *P. yoelii*. Together this data suggests that MBCs generated during primary infection with *P. yoelii* can differentiate into ASCs during secondary infection, and IgG-producing ASCs dominate the secondary response to *P. yoelii*. In comparison, we observed an expansion in B cells with a GC phenotype by day 5 p.c. However, it is unclear if MBCs are responsible for this increase.

IgM^{+} and $swIg^{+}$ *Plasmodium*-specific MBCs are capable of differentiating into ASCs and GC B cells upon reactivation.

The minimal expansion in Ag-specific IgM-secreting cells shortly after re-challenge indicates that the IgM^{+} MBCs may be non-responsive, possibly due to the high titers of MSP-1_{42}–specific

Abs still present in the serum before re-challenge, or they have the capacity to class switch and become IgG-secreting cells after reactivation. A third possibility is that they preferentially proceed to the GC. To explore these possibilities, we used an adoptive transfer approach. Using *P. yoelii* infected *aicda*^{cre}Ai6 reporter mice, IgM^{+} and swIg^{+} MBC populations expressing the ZsGreen1 protein as a surrogate for CD73 and CD80 co-expression (Fig. 1) were sorted and adoptively transferred into naïve congenic mice that were subsequently infected with *P. yoelii* (Fig. 6A). The functional capacity of the MBCs was evaluated 5, 8, and 28 days after infection.

Both MBC populations expanded after infection, as donor cell numbers significantly increased from day 5 to 8 (Fig. 6B). The vast majority of the recovered donor cells at the early time points after infection displayed a CD38$^{lo/-}$CD138^{+} phenotype indicative of plasmablasts (Fig. 6C,D), signifying that the transferred cells could differentiate into ASCs upon reactivation. The IgM^{+} MBCs that differentiated into plasmablasts lost their IgM expression (Fig. 6C,E), suggesting their ability to undergo class switch recombination. This was the case as congenic mice that received IgM^{+} MBCs had detectable Ag-specific IgG present in their serum compared to congenic mice that did not receive a donor cell transfer (Fig. 6F). Thus, IgM^{+} and swIg^{+} MBCs expand after reactivation and differentiate primarily into ASCs with the IgM^{+} MBCs undergoing class switch recombination following reactivation.

Transferred donor cells were still identifiable at day 28 p.i. and no difference in the number of recovered cells was seen between the donor groups (Fig. 7A,B). The majority of the donor cells displayed a GC B cell phenotype (CD38^{-}GL-7^{+}) at this time (Fig. 7A,C), indicating that IgM^{+} and swIg^{+} MBCs possess the ability to differentiate into GC B cells. Furthermore, Ag-specific MSP-1^{+} B cells were found amongst the donor-derived GC B cells from each transferred MBC population (Fig. 7A,D). Ag-specific IgG is readily detectable in the serum of congenic

mice that did not receive donor MBCs at this time. However, the impact of the transferred IgM$^+$ and swIg$^+$ MBCs was still observable, as higher titers of MSP-1 and AMA-1–specific IgG were present in these recipient mice (Fig. 7E). Overall, the transferred ZsGreen1$^+$ IgM$^+$ and IgG$^+$ MBCs displayed a similar function upon recall, differentiating into ASCs and GC B cells.

swIg$^+$ CD80$^-$CD73$^-$ MBCs are non-responsive to reactivation

While the above studies confirmed the function of the IgM$^+$ and swIg$^+$ CD80$^+$CD73$^+$ MBCs, they did not address the function of the swIg$^+$ CD80$^-$CD73$^-$ B cells, the other potential MBC population identified in mice after *P. yoelii* infection (Fig. 1). To address the role of these B cells, we attempted a similar approach, as shown in Figure 6. Instead, we sorted swIg$^+$ B cells that were either ZsGreen1$^+$ or ZsGreen1$^-$ and adoptively transferred them into congenic mice that were challenged with *P. yoelii*. We hypothesized if these B cells are indeed MBCs, then similar to the swIg$^+$ ZsGreen1$^+$ MBCs, they should favor differentiation into plasmablasts upon reactivation. However, if they behaved identical to the CD80$^-$PD-L2$^-$ MBCs described in other systems,[2] they should favor GC B cell development. Examination of the recovered CD45.2$^+$ enriched donor cells at day 8 and 28 p.i. indicated that the swIg$^+$ ZsGreen1$^+$ B cells maintained ZsGreen1 expression and, as seen before, were predominantly plasmablasts at day 8 p.i. and displayed a GC B cell phenotype at day 28 (Supplemental Fig. 4 and data not shown). In the case of the transferred swIg$^+$ ZsGreen1$^-$ B cells, poor recovery of these donor cells was seen at both time points, as cell numbers were never above the background amounts measured in the no transfer control groups. Furthermore, AID expression was not induced in the donor swIg$^+$ ZsGreen1$^-$ B cells as no ZsGreen1$^+$ B cells were recovered from the recipient mice (Supplemental Fig. 4).

The significantly reduced yields of recovered swIg$^+$ZsGreen1$^-$ MBCs may indicate that these B cells have a reduced fitness upon transfer into a naive host, possibly due to competition with naïve B cells for a survival signal. Therefore, as a separate approach to evaluate their function, swIg$^+$ZsGreen1$^-$ B cells and naïve and IgM$^+$ and swIg$^+$ ZsGreen$^+$ B cell populations were sorted from *aicda*^{cre}Ai6 reporter mice that recovered from a *P. yoelii* infection and restimulated in vitro. The IgM$^+$ MBCs and naïve B cells could differentiate into IgM-producing ASCs, and some of the secreted IgM was Ag-specific (Fig. 8A,B). As seen in vivo, a proportion of the IgM$^+$ MBCs could undergo class switch recombination after reactivation and differentiate into IgG-producing ASCs with some producing Ag-specific IgG (Fig. 8C,D). In contrast, the ability of naïve B cells to undergo class switch recombination and make IgG$^+$ ASCs during this stimulation period was reduced compared to the IgM$^+$ZsGreen1$^+$ MBCs, particularly their ability to produce Ag-specific IgG. As expected, the ability of the swIg$^+$ZsGreen1$^+$ to differentiate into IgG-producing ASCs was superior to the other B cell populations. However, the ability of IgM$^+$ and swIg$^+$ZsGreen1$^+$ MBCs to differentiate into Ag-specific IgG$^+$ ASCs was comparable across the mice (Fig. 8C,D). The swIg$^+$ZsGreen1$^-$ B cells responded poorly under the chosen in vitro stimulation conditions producing few to no IgG$^+$ ASCs. Together this data indicates that swIg$^+$ZsGreen1$^-$ B cells respond poorly to reactivation in vivo and in vitro, suggesting that these B cells are not true MBCs.

Discussion

Here, we indicate that MBC function upon recall with *P. yoelii* infection is not based on the isotype of the BCR, as IgM$^+$ and swIg$^+$ MBCs possessed the ability to differentiate into ASCs and GC B cells. These results contrast with the findings in other models that suggested that

reactivation of swIg$^+$ MBCs led predominantly to their differentiation into plasmablasts with very few producing GC B cells.[3,4] In both cases, mice were immunized with a non-replicating Ag. Hence, it is possible to speculate that the initial Ab burst due to the reactivation of transferred swIg$^+$ MBCs resulted in the secretion of enough IgG to clear the Ag in these models, thus, preventing MBCs from differentiating into GC B cells. Support for this idea comes from the Pape et al. study, where the reactivation of swIg$^+$ MBCs prevented the differentiation of endogenous B cells of the adoptive recipients from forming GCs.[4] Here, we utilized a replicating parasite to investigate MBC function, which results in the maintenance of Ag well beyond clearance of the infection, as seen by the presence of Ag-specific GC B cells at least 70 days after resolution of the infection (Fig. 3D). Thus, our observation of swIg$^+$ MBCs giving rise to B cells with a GC phenotype after transfer and challenge may be due in part to the inability of the Abs produced from MBC-derived plasmablasts to completely clear the parasite on their own. Thereby, a sufficient Ag load is available to allow for the accumulation of GC B cells.

Re-challenge of mice with *P. chabaudi* results in the rapid expansion of IgM-secreting plasmablasts, a proportion of which are T-cell independent.[40] In contrast, secondary infection with *P. yoelii* did not induce a substantial expansion in IgM-secreting plasmablasts, and instead, the secondary response was dominated by switched ASCs. The lack of expansion of IgM$^+$ MBCs seen here with *P. yoelii* mirrors the results seen with secondary immunization with PE, which the authors attributed to the high serum quantities of anti-PE IgG circulating in these mice before re-exposure to PE.[4] Similar to our findings here, the adoptive transfer of PE-specific IgM$^+$ MBCs into naïve mice that were subsequently immunized with PE showed that these cells could recognize and respond to PE in an environment lacking circulating anti-PE Abs, giving rise to swIg$^+$ ASCs and GC B cells.[4] Hence, we speculate that the ability of IgM$^+$ MBCs to expand in

response to secondary infection with *P. chabaudi* and not *P. yoelii* is due to differences in Ag-specific Ab quantity and/or quality in these mice at the time of re-infection. An idea supported by the differences in *P. yoelii* and *P. chabaudi* to establish secondary infections with blood parasitemia only detectable for the latter. *P. chabaudi* establishes a persistent infection after re-challenge, just as it did after primary infection but at a lower level of parasitemia.[58]

Thus, the Abs generated in response to primary infection with *P. yoelii* are more effective at preventing re-establishment of infection than those produced in response to *P. chabaudi* infection. Consequently, we speculate that critical epitopes recognized by the BCR of IgM^+ MBCs and naïve B cells are preferentially bound by affinity-matured circulating Ag-specific Abs or high-affinity BCRs associated with $swIg^+$ MBCs after re-infection with *P. yoelii*. In contrast, Ag is readily available for binding and reactivation of IgM^+ MBCs during secondary infection with *P. chabaudi*. The difference in the effectiveness of the Abs can be attributed to any number of factors, including increased titers and affinity of the Abs and differences in the production of Abs that target specific proteins essential for RBC binding and entry.

Importantly, our in vitro results indicate that the IgM^+ MBCs can give rise to Ag-specific IgM-secreting plasmablasts, meaning that these MBCs can respond to restimulation. However, in vivo, they favored differentiation into $swIg^+$ ASCs even in the absence of circulating Ag-specific Abs. Thus, additional factors such as inflammatory cytokines and additional signals derived from $CD4^+$ T cells may influence differentiation and class switching of IgM^+ MBCs after reactivation in the absence of Ag-specific Abs.

Instead of favoring a model where MBC isotype expression dictates effector function, our results favor a model in which the expression of specific cell surface proteins defines their functional activity. In this case, co-expression of $CD73^+$ and $CD80^+$ expression by IgM^+ and

swIg$^+$ MBCs represented a population of MBCs that had undergone extensive somatic hypermutation of their BCR and were capable of differentiating into ASCs and GC B cells. The ability of the CD73$^+$CD80$^+$ MBCs to yield swIg$^+$ ASCs during secondary responses echoed findings seen with CD80$^+$PD-L2$^+$ MBCs.[2] However, these CD80$^+$PD-L2$^+$ MBCs did not give rise to GC B cells regardless if they expressed IgM or if they were isotype-switched, which differed from the results seen here. Instead, populations of IgM-expressing CD80$^-$PD-L2$^-$ or CD80$^-$PD-L2$^+$ MBCs preferentially gave rise to secondary GC B cells. While abundantly found after NP-CGG immunization,[2,4] MBCs with a CD80$^-$PD-L2$^+$ phenotype were rarely present in the spleen after *P. yoelii* infection regardless of isotype expression, as most PD-L2$^+$ MBCs also expressed CD80 (Figure 1). Although IgM$^+$ CD73$^-$CD80$^-$ MBCs were indistinguishable from naïve B cells in this model, the swIg$^+$ CD73$^-$CD80$^-$ B cells found here did not respond to reactivation by differentiating into ASCs or GC B cells, indicating that these cells are not MBCs. The lack of somatic mutations in their BCR suggests that they are naive B cells that express IgD and low amounts of IgM. Another possibility is that these cells are anergic or in a transitional state following activation. Regardless of their origin or function, they are not a cell type contributing to the host's immediate protection upon re-infection.

The cell markers used by immunologists to identify MBC populations suggest that phenotypical and functional heterogeneity exists within the MBC pool. However, their biological function on MBCs remains to be defined. For instance, the ectoenzymes CD39 and CD73 are surface proteins involved in converting ATP to AMP and adenosine. Whereas CD39 is expressed on naïve B cells,[43] CD73 is upregulated on Ag-experienced and GC B cells,[5,54] and its expression is maintained on a subset of MBCs as seen here and by others.[2,5,13,14,40] Furthermore, Tfh cells express high amounts of CD73,[44] suggesting that the microenvironment of the GC is rich in

ATP. However, its role in the GC is still not understood, as germline deletion of CD73 does not impair the GC response and MBC formation in response to NP-CGG immunization.[44] Moreover, the mutational content of the BCR and MBC function in a recall response was not impacted by the loss of CD73. The only significant change observed in the absence of CD73 was reduced plasma cell accumulation in the bone marrow.[44] Therefore, it is unclear why MBCs maintain expression of this enzyme on their cell surface. Although work with human naïve B cells and IgM^+ MBCs showed that the ability of CD39 and CD73 to hydrolyze ATP to adenosine was required for class switch recombination.[59] Furthermore, patients with common variable immunodeficiency with impaired class-switched Ab responses possess B cells that are selectively deficient in CD73 expression.[59]

Signaling through the LIFR receptor on hematopoietic stem cells is required for their survival,[48] whether it promotes the survival of MBCs is unknown. However, the LIFR is functional on MBCs. They can respond to stimulation by LIFR agonists in vitro by inducing phosphorylation of Stat3.[41] MBCs are long-lived and can self-renew; therefore, they possess attributes associated with hematopoietic stem cells. Another subset of B cells that can self-renewal is B1 B cells. Interestingly, a subset of $CD25^+$ peritoneal B1 B cells was found to express the LIFR and are responsive to stimulation by LIF.[60] Thus, it is quite possible that LIF-LIFR signaling in MBCs plays a role in the maintenance of these cells, but further work is needed to address this possibility.

CCR6 expression is known to mark MBC precursors within the GC light zone; however, CCR6 expression is not required for MBC formation.[52] Here, we found the highest expression of CCR6 on $CD38^+GL\text{-}7^+$ B cells early after infection with *P. yoelii*. Though a small proportion of GC B cells expressed CCR6, only a tiny subset of $CD38^+GL\text{-}7^-$ B cells also expressed this

chemokine receptor, but they primarily did not co-express CD73. This result differs from the CD73$^+$ MBCs found in the Peyer's patch, where all IgA-bearing MBCs are positive for CCR6 and most express CD73 and PD-L2.[47] CCR6 expression not only regulated localization of MBCs within the Peyer's Patch but it also promoted their survival. The lack of CCR6 expression on the CD73$^+$ MBCs found here is intriguing given the additional finding that CCR6 expression is vital for the localization of MBCs in the spleen, but not their generation or maintenance.[50] Furthermore, altered localization of MBCs within the spleen impacts the ability of MBCs to be recalled to their cognate Ag in the absence of CCR6 expression, suggesting that the position of MBCs within the spleen is important for subsequent interactions with other cells such as T cells, which are implicated in the reactivation of some MBCs.[2,61] It is possible that infection with *P. yoelii,* as opposed to immunization with protein in adjuvant, leads to differences in CCR6 expression on MBCs observed in these models.

Although we found no evidence of rapid induction of IgM$^+$ MBCs into IgM-secreting cells, this does not diminish the potential importance of these cells to the recall response in humans. In particular, Ag-specific IgM$^+$ MBCs are identifiable in the blood of individuals from malaria-endemic regions,[37,40,62] and they can produce IgM Abs capable of neutralizing and promoting opsonization.[62] These Ag-specific IgM$^+$ MBCs were more abundant than their swIg$^+$ counterparts, even after years of repeated *Plasmodium* infections,[62] suggesting their capacity to play a protective role from severe disease and illustrating the inefficient acquisition of protective IgG responses against *Plasmodium*. Although, the reduced rate of somatically mutated BCRs in IgM$^+$ MBCs may make them better suited to recognize a broader range of variant *P. falciparum* Ags.

Lastly, as markers used to identify MBC populations continue to be defined and their function and biological role on MBCs is deduced, the challenge will be to determine if human MBCs similarly express these markers and if they display a similar functional role. Evidence of the expression of many of these markers on human MBCs is beginning to emerge. For instance, a recent study examining MBCs from patients with SAR-CoV-2 or acute *P. falciparum* malaria showed evidence of CD39 and CD73 expression by MBCs.[63] However, the frequency of cells expressing CD39 and CD73 was reduced in all MBC populations in the malaria patients but not the COVID-19 patients. Given a described role for CD73 in lymphocyte homing,[64] it is possible that the homing mechanism of MBCs is disrupted, or alternative receptors are used to promote homing into lymphoid tissues. It is also possible that given the link between CD73 and class switching,[59,65] reduction in adenosine production affects the ability of these MBCs to class switch upon reactivation. Further understanding of the functional role of proteins expressed on MBC populations may provide valuable insight into why B cells have difficulty building protective memory against *P. falciparum*.

Materials and Methods

Ethics statement

All animal studies described were done in concordance with the principles set forth by the Animal Welfare Act and the National Institutes of Health guidelines for the care and use of animals in biomedical research. All animal studies were reviewed and approved by the University of Arkansas for Medical Sciences Institutional Animal Care and Use Committee (Protocol number 3970).

Mice

Male and female B6.Cg-Gt(ROSA)26Sor$^{tm6(CAG-ZsGreen1)Hze}$/J (Ai6), B6.129P2-Aicda$^{tm(cre)Mnz}$/J (*aicda*^{cre}), B6.SJL-*Ptprc*^{a}*Pepc*^{b}/BoyJ (CD45.1) mice on a C57BL/6J background and WT C57BL/6J mice were obtained from The Jackson Laboratory. *Aicda*^{cre}Ai6 reporter mice were generated by breeding homozygous *aicda*^{cre} and Ai6 mice. Male BALB/c mice were obtained from Charles River Laboratories. All animals used in this study were between 7 and 12 weeks of age and were maintained and bred in specific pathogen-free facilities at the University of Arkansas for Medical Sciences in accordance with institutional guidelines.

Parasites

Male BALB/c mice were infected with frozen parasite stock of murine *Plasmodium yoelii* 17X (MRA-749, BEI Resources Repository, Manassas, VA). Subsequently, 10^5 parasitized erythrocytes derived from the passage were intraperitoneally (i.p.) injected into experimental groups of mice to establish infection. Mice were re-challenged at ≥ 90 days post-infection (p.i.) with 10^6 parasitized erythrocytes, i.p. Male and female mice were used for the described experiments (except for passaging parasite stock). During the primary infection, parasitemia was determined by flow cytometry as described,[66,67] or after re-challenge by Giemsa-stained thin-blood smears.

Flow cytometry and antibodies

Single-cell suspensions were obtained by passing the spleen through a 40 µm cell strainer followed by lysis of erythrocytes by re-suspension in a 0.86% NH_4Cl solution. Cells were maintained in complete RPMI (RPMI 1640 supplemented with 10% FBS, 10% sodium pyruvate, 10% non-

essential amino acids, 10% L-glutamine, 10% Pen/Strep, and 1% β-mercaptoethanol). 3-5 × 10^6 splenocytes from individual mice were aliquoted for staining into wells of a 96-well round-bottom plate. Cells were washed in FACS buffer (1 × PBS, 0.2% BSA and 0.2% 0.5M EDTA). Fc receptors were blocked in FACs buffer with anti-mouse CD16/32 (clone 24G2; BioXCell, Lebanon, NH) and normal mouse (ThermoFisher cat # 10410, Carlsbad, CA) and rat IgG (ThermoFisher cat # 10710C) in the presence of eF780 fixable viability dye (ThermoFisher cat # 65-0865-14). Surface staining was conducted with the following antibodies: CD73-PE-Cy7, GL-7-AF488, PD-L2-PE, IgM-BV710, B220-AF700, CD80-BV605, CCR6-APC, CD38-AF700, CD19-BV650, CD38-AF700, CD19-BV510, B220-BV650, CD73-BV605, B220-BV785, CD138-BV711, CD80-BV650, CD19-BV510, streptavidin-BV510 (BioLegend), LIFR-PE (R&D Systems, Minneapolis, MN), CD38-eF450, CD39-PcP-Cy5.5, CD80-FITC, IgM-APC, GL-7-eF450, IgD-biotin, CD3e-APC-eF780, CD11b-APC-eF780, CD11c-APC-eF780, Ter119-APC-eF780 (ThermoFisher). For samples that did not require intracellular staining, cells were fixed with 4% paraformaldehyde. Fluorescence minus one (FMO) controls were used to set the positive gates and indicate background staining for histogram plots. Samples were acquired on an LSRIIFortessa (BD Biosciences, San Jose, CA) and analyzed using FlowJo version X software (BD Biosciences, Ashland, OR).

Tetramer preparation

Recombinant His-tagged merozoite surface protein-1 (MSP-1_{42}) (amino acids 1398-1754; Accession P13828) and apical merozoite antigen-1 (AMA-1) (amino acids 26-478; Accession AAC47193) proteins from *P. yoelii* 17X were produced in *E. coli* as previously described.[68,69] After purification and refolding of MSP-1_{42} and AMA-1 proteins, the His-tag was cleaved using a

Thrombin kit (Millipore Sigma, St. Louis, MO). Confirmation of the His-tag removal was confirmed by W. blot using an anti-His Ab (ThermoFisher). MSP-1_{42} and AMA-1 were biotinylated and tetramerized with streptavidin-PE (SA-PE; Agilent, Santa Clara, CA) as previously described.[57] A decoy reagent to gate out the non-MSP-1_{42} or AMA-1–specific B cells was constructed by conjugating SA-PE to DyLight 650 (ThermoFisher) followed by washing and removal of any unbound DyLight 650 and incubating with an excess of biotin as described.[57]

Tetramer staining and enrichment

Single-cell suspensions of splenocytes were prepared as described above. Following red blood cell lysis, cells were resuspended in MACs buffer (Miltenyi BioTec, Bergisch Gladbach, Germany), and Fc receptors were blocked with anti-mouse CD16/32 (24G2; BioXCell) in a buffer containing normal mouse and rat IgG (ThermoFisher) for 20 minutes at 4°C. Then 10 nM of the prepared decoy reagent was incubated with the cells for 5 minutes at room temperature. MSP-1 or AMA-1–PE tetramers were then added at a concentration of 10 nM of SA, and the cells were incubated at 4°C for 30 minutes. Cells were subsequently washed in MACs buffer before incubating with anti-PE microbeads (Miltenyi) for 5 minutes at 4°C. Cells were once again washed in MACs buffer prior to positive selection on an AutoMACS Pro cell separator (Miltenyi). Recovered cells were surface stained and ran on a BD LSRIIFortessa. Collected data were analyzed using FlowJo version X software.

BCR sequencing

MSP-1_{42} and AMA-1 tetramer-specific MBCs were sorted from day 90 *P. yoelii* or naïve *aicda*^{cre}Ai6 reporter mice. Cells were pooled from the spleens of three individual mice then sub-

gated based on the following parameters: live, single cells, decoy$^-$tetramer$^+$CD19$^+$B220$^+$ and sorted as follows: CD38$^+$GL-7$^-$IgM$^+$ZsGreen1$^-$ naïve B cells, CD38$^+$GL-7$^-$IgM$^+$ZsGreen1$^+$, CD38$^+$GL-7$^-$swIg$^+$ZsGreen1$^+$, and CD38$^+$GL-7$^-$swIg$^+$ZsGreen1$^-$ B cells. cDNA from individual B cells was used to generate a V(D)J library using a kit from 10x Genomics (Pleasanton, CA). Libraries were sequenced on a NextSeq 150-cycle high-output flow cell (Illumina, San Diego, CA). The Loupe V(D)J Browser (10x Genomics) was used to identify somatic mutations in the heavy and light chain genes of individual B cells. Individual V_H and V_L chain sequences were cross-checked and confirmed using the NCBI's IgBLAST tool.

Adoptive transfer experiments

Aicda^{cre}Ai6 mice were sacrificed at least 70 days after infection with *P. yoelii* 17X parasites. Spleens were harvested and enriched for B cells by depleting other immune cell populations after labeling with biotinylated Abs against CD11b, CD3ε, Ter119 and CD11c followed by incubation with SA microbeads (Miltenyi Biotech) on an AutoMACS Pro cell separator (Miltenyi Biotech). Negative fractions were combined and stained to identify populations of MBCs. Live, single-cell CD19$^+$B220$^+$CD38$^+$GL7$^-$ MBCs were sorted based on the following parameters: IgM$^+$ (ZsGreen1$^+$IgG$^-$), or swIg$^+$ (ZsGreen1$^+$IgM$^-$ or ZsGreen1$^-$IgM$^-$) using a BD Biosciences FACSAria. FACS sorted cells were rested in cRPMI at 37°C for at least 30 minutes before prepping the cells for transfer. Cells were washed two times in sterile 1 × PBS and then resuspended in sterile 1 × PBS. Cells were loaded into a 1ml syringe with a 30-gauge needle. Approximately 4-8 × 10^4 ZsGreen1$^+$IgM$^+$, ZsGreen1$^+$swIg$^+$ or ZsGreen1$^-$swIg$^+$ MBCs were transferred via the retro-orbital sinus into congenic CD45.1$^+$ mice. Mice were challenged with 10^5 *P. yoelii* pRBCs i.p. the following day. Transferred cells were recovered from infected mice on

day 5, 8, or 28 p.i. by first staining with anti-CD45.2-PE and then enriched with the use of anti-PE microbeads (Miltenyi Biotech) followed by positive selection on an autoMACs Pro Separator.

ELISAs

High binding Immunlon HBX plates (ThermoFisher) were coated with 2.5μg/ml of recombinant *P. yoelii* AMA-1 or MSP-1_{42} proteins in sodium bicarbonate buffer overnight at 4°C. Plates were blocked with 5% FBS (ThermoFisher) or FetalPlex (Gemini Bio, Calabasas, CA) in PBS for one hour at 37°C. Serum isolated from mice was initially diluted 1:50 and then serially diluted 1:3 down the plate leaving the last row for blocking buffer to serve as the blank control. HRP-conjugated IgG or IgM (Southern Biotech, Birmingham, AL) was incubated on the plate for 1h at 37°C, and SureBlue substrate (Sera care, Milford, MA) was used for detection. The reactions were neutralized with stop solution (Sera care) before reading plates. The plates were read on a FLUOStar Omega plate reader (BMG Labtech, Offenburg, Germany) at an absorbance of 450 nm.

ELISpot assays

Briefly, following activation with 35% EtOH ELISpot plates (Millipore cat # MAHAS4510) were coated overnight at 4°C with 2.5 μg/ml of *P. yoelii* recombinant MSP-1_{42} or AMA-1 protein in PBS. The following day, the plates were blocked for 30 minutes at room temperature with cRPMI. Afterward, 10^5 splenocytes were plated and incubated overnight at 37°C in cRPMI. Plates were washed with PBS and then blocked with 5% FBS in PBS for 1 h at room temperature. Secondary IgM-AP (SouthernBiotech cat # 1020-04) or IgG-AP (SouthernBiotech cat # 1030-04) conjugated Abs were then incubated for 1 hour at 37°C in 5% FBS in PBS. Finally, an ELISpot developing reagent (consisting of BCIP and NBT; Sigma Millipore) was used to visualize spots; subsequently,

an AID ELISpot reader system (Autoimmun Diagnostika, Strassberg, Germany) was utilized to calculate the number of ASCs.

For the MBC ELISpot assays, sorted populations of MBCs (ZsGreen1$^-$IgM$^+$, ZsGreen1$^-$swIg$^+$, ZsGreen1$^+$IgM$^+$ or ZsGreen1$^+$swIg$^+$) were plated at a concentration of 5,000/well in 96-well round-bottom plates. MBCs were restimulated in the presence of the TLR7 agonist R848 (1 μg/ml; Invivogen, San Diego, CA) and human IL-2 (10 ng/ml; Peprotech, Rocky Hill, NJ) with or without splenic feeder cells depleted of B cells (50,000/well). Splenic feeder cells incubated with R848 and human IL-2 and MBCs incubated without restimulation or added splenic feeder cells served as controls. Cells were incubated in vitro for three days at 37°C. After three days, the cells were transferred to ELISpot plates pre-coated with 2.5 μg/ml of *P. yoelii* recombinant MSP-1_{42} and AMA-1 or 10 μg/ml anti-mouse Kappa (Southern Biotech). Cells were incubated for 16-24 h at 37°C. Spots were visualized as described above.

Statistics

Unless otherwise noted in the figure legend, Individual *p*-values for each associated statistical test are listed in the figure legends. GraphPad Prism 9 (San Diego, CA) was used for all statistical analyses.

Acknowledgments

Plasmodium yoelii 17X was obtained through BEI Resources, NIAID, NIH: MRA-749, contributed by D. Walliker. Special thanks to Andrea Harris for her technical assistance as part of the flow cytometry core.

Funding

This work was supported by the Arkansas Biosciences Institute and National Institutes of Health (NIH) Grant AI116653 (J.S.S.) and P20-GM103625-Project 3 (to J.S.S.). The flow cytometry core is supported by the Translational Research Institute (Grant UL1-TR000039; NIH National Center for Research Resources and National Center for Advancing Translation Sciences) and the UAMS Center for Microbial Pathogenesis and Host Inflammatory Responses (Grant P20-GM103625; NIH National Institute of General Medical Sciences Centers of Biomedical Research Excellence).

Author Contribution

Conceived and designed the experiments: JSS. Performed the experiments: SLB, JJB, JL, EN. Analyzed the data: SLB, JJB, JSS. Wrote the paper: JSS.

Conflict of Interest

The authors report no conflict of interest.

References

1. Anderson SM, Tomayko MM, Shlomchik MJ. Intrinsic properties of human and murine memory B cells. *Immunol Rev*. 2006;211:280–294.

2. Zuccarino-Catania GV, Sadanand S, Weisel FJ, et al. CD80 and PD-L2 define functionally distinct memory B cell subsets that are independent of antibody isotype. *Nat Immunol*. 2014;15:631 637.

3. Dogan I, Bertocci B, Vilmont V, et al. Multiple layers of B cell memory with different effector functions. *Nat Immunol*. 2009;10:1292–1299.

4. Pape KA, Taylor JJ, Maul RW, et al. Different B Cell Populations Mediate Early and Late Memory During an Endogenous Immune Response. *Science*. 2011;331:1203–1207.

5. Taylor JJ, Pape KA, Jenkins MK. A germinal center–independent pathway generates unswitched memory B cells early in the primary response. *J Exp Medicine*. 2012;209:597–606.

6. Obukhanych TV, Nussenzweig MC. T-independent type II immune responses generate memory B cells. *J Exp Medicine*. 2006;203:305–310.

7. Shlomchik MJ. Do Memory B Cells Form Secondary Germinal Centers? *Csh Perspect Biol*. 2018;10:a029405.

8. Pape KA, Jenkins MK. Do Memory B Cells Form Secondary Germinal Centers? *Csh Perspect Biol*. 2018;10:a029116.

9. McHeyzer-Williams LJ, Dufaud C, McHeyzer-Williams MG. Do Memory B Cells Form Secondary Germinal Centers? *Csh Perspect Biol*. 2018;10:a028878.

10. Weill J-C, Gallou SL, Hao Y, et al. Multiple players in mouse B cell memory. *Curr Opin Immunol*. 2013;25:334–338.

11. Mesin L, Schiepers A, Ersching J, et al. Restricted Clonality and Limited Germinal Center Reentry Characterize Memory B Cell Reactivation by Boosting. *Cell*. 2019;180:92-106.e11.

12. McHeyzer-Williams LJ, Milpied PJ, Okitsu SL, et al. Class-switched memory B cells remodel BCRs within secondary germinal centers. *Nat Immunol*. 2015;16:296 305.

13. Anderson SM, Tomayko MM, Ahuja A, et al. New markers for murine memory B cells that define mutated and unmutated subsets. *J Exp Medicine*. 2007;204:2103–2114.

14. Tomayko MM, Steinel NC, Anderson SM, et al. Cutting Edge: Hierarchy of Maturity of Murine Memory B Cell Subsets. *J Immunol*. 2010;185:7146–7150.

15. Metzger WG, Okenu DMN, Cavanagh DR, et al. Serum IgG3 to the Plasmodium falciparum merozoite surface protein 2 is strongly associated with a reduced prospective risk of malaria. *Parasite Immunol*. 2003;25:307 312.

16. McGregor IA. The Passive Transfer of Human Malarial Immunity. *Am J Trop Med Hyg*. 1964;13:SUPPL 237 9.

17. Cohen S, McGregor IA, Carrington S. Gamma-globulin and acquired immunity to human malaria. *Nature*. 1961;192:733 737.

18. Riley EM, Allen SJ, Wheeler JG, et al. Naturally acquired cellular and humoral immune responses to the major merozoite surface antigen (PfMSP1) of Plasmodium falciparum are associated with reduced malaria morbidity. *Parasite Immunol*. 1992;14:321 337.

19. Osier FHA, Murungi LM, Fegan G, et al. Allele-specific antibodies to Plasmodium falciparum merozoite surface protein-2 and protection against clinical malaria. *Parasite Immunol*. 2010;32:193–201.

20. Weid T von der, Honarvar N, Langhorne J. Gene-targeted mice lacking B cells are unable to eliminate a blood stage malaria infection. *Journal of immunology*. 1996;156:2510 2516.

21. Grun JL, Weidanz WP. Immunity to Plasmodium chabaudi adami in the B-cell-deficient mouse. *Nature*. 1981;290:143 145.

22. Weinbaum FI, Evans CB, Tigelaar RE. Immunity to Plasmodium Berghei yoelii in mice. I. The course of infection in T cell and B cell deficient mice. *J Immunol Baltim Md 1950*. 2012;117:1999–2005.

23. Langhorne J, Cross C, Seixas E, et al. A role for B cells in the development of T cell helper function in a malaria infection in mice. *Proc Natl Acad Sci U S A*. 1998;95:1730 1734.

24. Meding SJ, Langhorne J. CD4+ T cells and B cells are necessary for the transfer of protective immunity to Plasmodium chabaudi chabaudi. *Eur J Immunol*. 1991;21:1433–8.

25. Portugal S, Pierce SK, Crompton PD. Young Lives Lost as B Cells Falter: What We Are Learning About Antibody Responses in Malaria. *J Immunol*. 2013;190:3039–3046.

26. Ly A, Hansen DS. Development of B Cell Memory in Malaria. *Front Immunol*. 2019;10:559.

27. Struik SS, Riley EM. Does malaria suffer from lack of memory? *Immunol Rev*. 2004;201:268 290.

28. Achtman AH, C. B P, Stephens R, et al. Longevity of the immune response and memory to blood-stage malaria infection. *Current topics in microbiology and immunology*. 2005;297:71 102.

29. Ndungu FM, Olotu A, Mwacharo J, et al. Memory B cells are a more reliable archive for historical antimalarial responses than plasma antibodies in no-longer exposed children. *Proc National Acad Sci*. 2012;109:8247 8252.

30. Wipasa J, Suphavilai C, Okell LC, et al. Long-lived antibody and B Cell memory responses to the human malaria parasites, Plasmodium falciparum and Plasmodium vivax. *Plos Pathog*. 2010;6:e1000770.

31. Nogaro SI, Hafalla JC, Walther B, et al. The Breadth, but Not the Magnitude, of Circulating Memory B Cell Responses to P. falciparum Increases with Age/Exposure in an Area of Low Transmission. *Plos One*. 2011;6:e25582.

32. Changrob S, McHenry AM, Nyunt MH, et al. Persistence of Long-lived Memory B Cells specific to Duffy Binding Protein in individuals exposed to Plasmodium vivax. *Sci Rep-uk*. 2018;8:8347.

33. Wykes MN, Zhou YH, Liu XQ, et al. Plasmodium yoelii can ablate vaccine-induced long-term protection in mice. *J Immunol*. 2005;175:2510 2516.

34. Xu H, Wipasa J, Yan H, et al. The mechanism and significance of deletion of parasite-specific CD4(+) T cells in malaria infection. *The Journal of experimental medicine*. 2002;195:881 892.

35. Weiss GE, Traore B, Kayentao K, et al. The Plasmodium falciparum-Specific Human Memory B Cell Compartment Expands Gradually with Repeated Malaria Infections. *Plos Pathog*. 2010;6:e1000912 13.

36. Dorfman JR, Bejon P, Ndungu FM, et al. B cell memory to 3 Plasmodium falciparum blood-stage antigens in a malaria-endemic area. *J Infect Dis*. 2005;191:1623 1630.

37. Triller G, Scally SW, Costa G, et al. Natural Parasite Exposure Induces Protective Human Anti-Malarial Antibodies. *Immunity*. 2017;47:1197-1209.e10.

38. Nduati EW, Ng DHL, Ndungu FM, et al. Distinct kinetics of memory B-cell and plasma-cell responses in peripheral blood following a blood-stage Plasmodium chabaudi infection in mice. *Plos One*. 2010;5:e15007.

39. Ndungu FM, Cadman ET, Coulcher J, et al. Functional memory B cells and long-lived plasma cells are generated after a single Plasmodium chabaudi infection in mice. *Plos Pathog*. 2009;5:e1000690.

40. Krishnamurty AT, Thouvenel CD, Portugal S, et al. Somatically Hypermutated Plasmodium-Specific IgM+ Memory B Cells Are Rapid, Plastic, Early Responders upon Malaria Rechallenge. *Immunity*. 2016;45:402–414.

41. Tomayko MM, Anderson SM, Brayton CE, et al. Systematic Comparison of Gene Expression between Murine Memory and Naive B Cells Demonstrates That Memory B Cells Have Unique Signaling Capabilities. *J Immunol*. 2008;181:27 38.

42. Bhattacharya D, Cheah MT, Franco CB, et al. Transcriptional Profiling of Antigen-Dependent Murine B Cell Differentiation and Memory Formation. *J Immunol*. 2007;179:6808–6819.

43. Kaku H, Cheng KF, Al-Abed Y, et al. A Novel Mechanism of B Cell–Mediated Immune Suppression through CD73 Expression and Adenosine Production. *J Immunol*. 2014;193:5904–5913.

44. Conter LJ, Song E, Shlomchik MJ, et al. CD73 Expression Is Dynamically Regulated in the Germinal Center and Bone Marrow Plasma Cells Are Diminished in Its Absence. *Plos One*. 2014;9:e92009 10.

45. Good-Jacobson KL, Song E, Anderson S, et al. CD80 Expression on B Cells Regulates Murine T Follicular Helper Development, Germinal Center B Cell Survival, and Plasma Cell Generation. *J Immunol*. 2012;188:4217–4225.

46. Good-Jacobson KL, Szumilas CG, Chen L, et al. PD-1 regulates germinal center B cell survival and the formation and affinity of long-lived plasma cells. *Nat Immunol*. 2010;11:535.

47. Lin Y-L, Ip P-P, Liao F. CCR6 Deficiency Impairs IgA Production and Dysregulates Antimicrobial Peptide Production, Altering the Intestinal Flora. *Front Immunol*. 2017;8:805.

48. Escary JL, Perreau J, Duménil D, et al. Leukaemia inhibitory factor is necessary for maintenance of haematopoietic stem cells and thymocyte stimulation. *Nature*. 1993;363:361 364.

49. Salazar-Gonzalez RM, Niess JH, Zammit DJ, et al. CCR6-Mediated Dendritic Cell Activation of Pathogen-Specific T Cells in Peyer's Patches. *Immunity*. 2006;24:623–632.

50. Elgueta R, Marks E, Nowak E, et al. CCR6-Dependent Positioning of Memory B Cells Is Essential for Their Ability To Mount a Recall Response to Antigen. *J Immunol*. 2015;194:505–513.

51. Faas MM, Sáez T, Vos P de. Extracellular ATP and adenosine: The Yin and Yang in immune responses? *Mol Aspects Med*. 2017;55:9–19.

52. Suan D, Kräutler NJ, Maag JLV, et al. CCR6 Defines Memory B Cell Precursors in Mouse and Human Germinal Centers, Revealing Light-Zone Location and Predominant Low Antigen Affinity. *Immunity*. 2017;47:1142 1153.e4.

53. Ying Q-L, Nichols J, Chambers I, et al. BMP Induction of Id Proteins Suppresses Differentiation and Sustains Embryonic Stem Cell Self-Renewal in Collaboration with STAT3. *Cell*. 2003;115:281–292.

54. Kaji T, Ishige A, Hikida M, et al. Distinct cellular pathways select germline-encoded and somatically mutated antibodies into immunological memory. *J Exp Medicine*. 2012;209:2079–2097.

55. Madisen L, Zwingman TA, Sunkin SM, et al. A robust and high-throughput Cre reporting and characterization system for the whole mouse brain. *Nat Neurosci*. 2010;13:133 140.

56. Robbiani DF, Bothmer A, Callen E, et al. AID is required for the chromosomal breaks in c-myc that lead to c-myc/IgH translocations. *Cell*. 2008;135:1028 1038.

57. Taylor JJ, Martinez RJ, Titcombe PJ, et al. Deletion and anergy of polyclonal B cells specific for ubiquitous membrane-bound self-antigen. *J Exp Medicine*. 2012;209:2065–2077.

58. Latham LE, Wikenheiser DJ, Stumhofer JS. ICOS signaling promotes a secondary humoral response after re-challenge with Plasmodium chabaudi chabaudi AS. *Plos Pathog*. 2020;16:e1008527.

59. Schena F, Volpi S, Faliti CE, et al. Dependence of Immunoglobulin Class Switch Recombination in B Cells on Vesicular Release of ATP and CD73 Ectonucleotidase Activity. *Cell Reports*. 2013;3:1824–1831.

60. Tumang JR, Holodick NE, Vizconde TC, et al. A CD25− Positive Population of Activated B1 Cells Expresses LIFR and Responds to LIF. *Front Immunol*. 2011;2:6.

61. Ise W, Inoue T, McLachlan JB, et al. Memory B cells contribute to rapid Bcl6 expression by memory follicular helper T cells. *Proc National Acad Sci*. 2014;111:11792–11797.

62. Hopp CS, Diouf A, Miura K, et al. Plasmodium falciparum-specific IgM B cells dominate in children, expand with malaria and produce parasite inhibitory IgM. *Biorxiv*. 2020;2020.04.12.030049.

63. Wildner NH, Ahmadi P, Schulte S, et al. B cell analysis in SARS-CoV-2 versus malaria: Increased frequencies of plasmablasts and atypical memory B cells in COVID-19. *J Leukocyte Biol*. 2021;109:77–90.

64. Takedachi M, Qu D, Ebisuno Y, et al. CD73-Generated Adenosine Restricts Lymphocyte Migration into Draining Lymph Nodes. *J Immunol*. 2008;180:6288–6296.

65. Kim E, Ackermann C, Tóth I, et al. Down-regulation of CD73 on B cells of patients with viremic HIV correlates with B cell activation and disease progression. *J Leukocyte Biol*. 2017;101:1263–1271.

66. Wikenheiser DJ, Brown SL, Lee J, et al. NK1.1 Expression Defines a Population of CD4+ Effector T Cells Displaying Th1 and Tfh Cell Properties That Support Early Antibody Production During Plasmodium yoelii Infection. *Front Immunol*. 2018;9:2277.

67. Malleret B, Claser C, Ong ASM, et al. A rapid and robust tri-color flow cytometry assay for monitoring malaria parasite development. *Sci Rep-uk*. 2011;1:118.

68. Shi Q, Lynch MM, Romero M, et al. Enhanced Protection against Malaria by a Chimeric Merozoite Surface Protein Vaccine ▿ . *Infect Immun*. 2007;75:1349–1358.

69. Burns JM, Flaherty PR, Romero MM, et al. Immunization against Plasmodium chabaudi malaria using combined formulations of apical membrane antigen-1 and merozoite surface protein-1. *Vaccine*. 2003;21:1843–1852.

Figure Legends

Figure 1 MBCs form a heterogeneous population after *P. yoelii* infection. (A-G) C57BL/6 mice were infected with *P. yoelii* 17X. (A) Representative flow plots of CD73 and CD80 expression on IgM^+ or $swIg^+$ $CD38^+GL\text{-}7^-$ B cells at various times after *P. yoeli*i infection. (B) Total number of IgM^+ and $swIg^+$ $CD73^+CD80^+$ and $CD73^-CD80^-$ $CD38^+GL\text{-}7^-$ B cells over 350 days p.i. (C) Representative flow plots of PD-L2 expression on IgM^+ and $swIg^+$ $CD73^+CD80^+$ and $CD73^-CD80^-$ B cells at day 167 p.i. (D) Total number of IgM^+ and $swIg^+$ $CD73^+CD80^+PD\text{-}L2^+$ $CD38^+GL\text{-}7^-$ B cells over 350 days p.i. (E) Representative flow plots of CD39 and CD73 expression on IgM^+ and $swIg^+$ $CD38^+GL\text{-}7^-$ B cells at day 28 p.i. (F) Total number of IgM^+ and $swIg^+$ $CD73^+CD39^+$ $CD38^+GL\text{-}7^-$ B cells over 167 days p.i. (G) Representative histogram of CCR6 expression on $CD38^+GL\text{-}7^+$ B cells (solid black line), $swIg^+$ (light gray shaded) and IgM^+ (dotted black line) $CD38^+GL\text{-}7^-$ B cells at day 7 p.i. CCR6 FMO (dark gray shaded). Graph denoting CCR6 median fluorescence intensity (MFI) on splenic B cell populations at select times after *P. yoelii* infection. (H) Representative flow plots of CCR6 expression on IgM^+ and $swIg^+$ $CD38^+GL\text{-}7^-$ B cells at day 28 p.i. (I) Representative histogram plots of LIFR expression on IgM^+ and $swIg^+$ $CD73^+CD80^+$ (solid black line) and $CD73^-CD80^-$ (dotted black line) $CD38^+GL\text{-}7^-$ B cells at day 28 p.i. LIFR FMO (gray shaded). Graph showing the frequency of LIFR expression on MBC populations at day 28 p.i. (B,D,F) Each data point shows the mean ± S.E.M. with 3-6 mice per time point. Representative of three independent experiments. (G,I) Each point represents an individual mouse, and the error bars denote the mean ± S.E.M. Data are representative of three independent experiments with n = 3 mice per group.

Figure 2 ZsGreen1 fluorescence can serve as a surrogate to mark CD73$^+$CD80$^+$ MBCs. *Aicda*^{cre}Ai6 reporter mice were infected with *P. yoelii*. (A) Representative flow plots of ZsGreen1 expression in IgM$^+$ and swIg$^+$ CD73$^-$CD80$^-$ and CD73$^+$CD80$^+$ CD38$^+$GL-7$^-$ B cells at day 167 p.i. (B) Frequency of ZsGreen1 expression in IgM$^+$ and swIg$^+$ CD73$^-$CD80$^-$ and CD73$^+$CD80$^+$ CD38$^+$GL-7$^-$ B cells at day 167 p.i. Each point represents an individual mouse, and the error bars denote the mean ± S.E.M. Data are representative of three independent experiments with n = 3-4 mice per group.

Figure 3 Identification and kinetics of MSP-1–specific B cells using a B cell tetramer. (A) Representative flow plot showing gated splenic B cell populations identified after excluding dead cells, doublets, and non-B cells (CD3$^+$CD11b$^+$Ter119$^+$) and enrichment with MSP-1 and decoy tetramers. Representative flow plots showing gating of MSP-1$^+$decoy$^-$ B cells from naïve and C57BL/6 mice infected for 7 days with *P. yoelii*. (B) Total number of MSP-1$^+$ B cells over 365 days p.i. (C) Representative flow plots identifying CD138$^+$MSP-1$^+$ plasmablasts (left), CD138$^-$CD19$^+$MSP-1$^+$ B cells (middle), and CD38$^+$GL-7$^-$ (memory/naïve), CD38$^+$GL-7$^+$ (precursor), and CD38$^-$GL-7$^+$ (GC) B cells sub-gated from the CD138$^-$CD19$^+$MSP-1$^+$ B cells (right). (D) Total number of MSP-1$^+$ plasmablasts, memory/naïve, and GC B cells over 365 days p.i. (B,D) Each data point shows the mean ± S.E.M. with 7-15 mice per time point. Data are combined from three independent experiments.

Figure 4 MSP-1–specific MBCs are phenotypically and genetically distinct populations. (A) Representative gating strategy used to identify MSP-1$^+$ isotype switched and IgM$^+$ MBCs based on CD73 and CD80 staining at day 70 p.i. Total number of MSP-1$^+$ swIg$^+$ or IgM$^+$ (B)

$CD73^+CD80^+$ or (C) $CD73^-CD80^-$ MBCs over 365 days p.i. Each data point shows the mean ± S.E.M. with 7-15 mice per time point. Data are combined from three independent experiments. Total number of mutations found in the CDR1 and CDR2 of the (D) heavy and (E) light chain gene of individual MSP-1–specific B cell clones. Numbers in parentheses represent the number of individual B cell clones assessed and graphed for each population. Dark dotted line in the violin plot represents the median, while the light dashed lines represent the quartiles. Significance was calculated by one-way ANOVA Kruskal-Wallis test with post hoc Dunn's multiple comparisons test. **** $p < 0.0001$. (F) Frequency of IgG subclasses used by individually sequenced $ZsGreen1^+swIg^+$ MBC clones.

Figure 5 IgG^+ ASCs dominate the secondary response to *P. yoelii*. (A) Representative flow plots identifying MSP-1–specific $CD138^+$ plasmablasts and $CD19^+$ B cells before and after re-challenge of mice at day 90 p.i. with 10^6 *P. yoelii* infected RBCs. (B) Total number of MSP-1^+ B cells before and after re-challenge. (C) Total number of MSP-1^+ naïve/MBCs, GC B cells, and plasmablasts before and after re-challenge. (D) Serum IgM and IgG titers specific for MSP-1 were determined by ELISA. (E) Splenocytes isolated before re-challenge (day 90) and post-challenge (days 3, 5, and 9) were used to determine the number of MSP-1-specific IgM and IgG ASCs by ELISpot. (B,C,E) Each point represents an individual mouse, and the error bars denote the mean ± S.E.M. with 5 mice per time point. Data are representative of three independent experiments. (B,C,D) Significance was calculated by one-way ANOVA Kruskal-Wallis test with post hoc Dunn's multiple comparisons test. (E) Significance was calculated by two-way ANOVA with post hoc Holm-Sidak's multiple comparisons test. *$p < 0.05$, **$p < 0.01$, ***$p < 0.001$, ****$p < 0.0001$, $^{\#}p < 0.05$, $^{\#\#}p < 0.01$. In **D,** the absorbance values for each dilution for

the post-challenge samples were compared against the absorbance values for the pre-challenge samples. # represents the comparison between pre-challenge and day 5 p.c., and * represents the comparison between pre-challenge and day 9 p.c.

Figure 6 ZsGreen1$^+$IgM$^+$ MBCs predominantly differentiate into class switched ASCs after reactivation. (A) Experimental model. ZsGreen1$^+$ IgM$^+$ or swIg$^+$ MBCs were enriched and sorted from *aicda*^{cre}Ai6 reporter mice ≥ 70 days after infection. 4-8 × 10^4 MBCs were transferred into naïve congenic CD45.1$^+$ mice that were challenged 24 h later with 10^5 *P. yoelii* infected RBCs. Donor cells were recovered 5, 8, and 28 days after challenge. (B) Total number of recovered donor cells at day 5 and 8 p.i. (C) Representative flow plots from day 8 p.i. showing gating strategy to identify CD45.2$^+$ZsGreen1$^+$ donor cells (left). Recovered donor cells were analyzed for their ability to differentiate into CD138$^+$CD38$^{lo/-}$ plasmablasts (middle) and the expression of IgM on the plasmablasts (right). Gates in middle and right plots based on the endogenous B cell population in the recipient mice. (D) Frequency of plasmablasts found within the recovered donor cell populations. (E) Frequency of IgM$^+$ plasmablasts found within the recovered ZsGreen1$^+$IgM$^+$ donor cells. (F) Serum IgG titers specific for MSP-1 and AMA-1 were determined by ELISA from day 8 infected mice. Samples were combined from three independent experiments. (B,D,E) Each point represents an individual mouse, and the error bars denote the mean ± S.E.M. with 3-4 mice per time point. Data are representative of three independent experiments. Significance was calculated by one-way ANOVA Kruskal-Wallis test with post hoc Dunn's multiple comparisons test. *$p < 0.05$. In **F,** the absorbance values for each dilution for the transfer recipient samples were compared against the absorbance values for the no transfer recipient samples. * represents the comparison between swIg$^+$ donors and no transfer.

Figure 7 ZsGreen1$^+$ IgM$^+$ and swIg$^+$ MBCs can differentiate into GC B cells after reactivation. Representative flow plots from day 28 p.i. showing gating strategy to identify CD45.2$^+$ZsGreen1$^+$ donor cells (left). Recovered donor cells were analyzed for their ability to differentiate into CD38$^-$GL-7$^+$ GC B cells or retain their CD38$^+$GL-7$^-$ MBC phenotype (middle). Donor cells that displayed a GC phenotype were subsequently analyzed to determine their ability to bind MSP-1 (right). (B) Total number of recovered donor cells at day 28 p.i. (C) Frequency of GC B cells found within the recovered donor cell populations. (D) Frequency of GC B cells that specifically bound MSP-1 found within the recovered donor cell populations. (E) Serum IgG titers specific for MSP-1 and AMA-1 were determined by ELISA from day 28 infected mice. Samples were combined from two independent experiments. (B,C,D) Each point represents an individual mouse, and the error bars denote the mean ± S.E.M. with 4-5 mice per group. Data are representative of three independent experiments. Significance was calculated by one-way ANOVA Kruskal-Wallis test with post hoc Dunn's multiple comparisons test. In **E,** the absorbance values for each dilution for the transfer recipient samples were compared against the absorbance values for the no transfer recipient samples.

Figure 8 Stimulation of swIg$^+$ CD80$^-$CD73$^-$ B cells in vitro does not induce their differentiation into ASCs. Splenocytes from *aicda*^{cre}Ai6 reporter were isolated ≥ day 90 p.i to enrich and sort populations of MBCs based on the presence or absence of ZsGreen1 expression and the presence or absence of IgM$^+$ expression to determine their ability to differentiate into ASCs after restimulation in vitro. Sorted populations of MBCs were left unstimulated or restimulated with the TLR7 agonist R848 in the presence of IL-2 with or without B cell-depleted

splenic feeder cells. (A) Total IgM^+ or (B) IgM^+ MSP-1/AMA-1–specific ASCs and (C) total IgG^+ or (D) IgG^+ MSP-1/AMA-1–specific ASCs were determined by ELISpot. Each point represents an individual mouse, and the error bars denote the mean ± S.E.M. Data are representative of three combined experiments with an n = 9 mice. Significance was calculated by two-way ANOVA with post hoc Holm-Sidak's multiple comparisons test. $*p < 0.05$, $**p < 0.01$, $***p < 0.001$, $****p < 0.0001$.

Supplemental Figure 1 Gating strategy used to denote different B cell populations in the spleen. (A) Experimental model used in figures 1-4 and supplemental figures 1-3. C57BL/6 or *aicda*^{cre}Ai6 reporter mice were infected with 10^5 *P. yoelii* infected RBCs. Splenic B cell populations were analyzed by flow cytometry at indicated times p.i. after excluding dead cells, doublets, and non-B cells ($CD3^+CD11b^+Ter119^+$). (B) Representative flow plots from day 70 p.i. displaying the gating strategy used to identify IgM^+ and $swIg^+$ MBCs based on CD73 and CD80 expression patterns. (C) Representative flow plots showing the gates used to distinguish the IgD^{hi} and $IgD^{lo/-}$ B cells within the IgM^+ and $swIg^+$ $CD73^+CD80^+$ and $CD73^-CD80^-$ MBC pools at day 54 p.i. The graph displays the frequency of IgD^{hi} B cells amongst MBC populations at day 54 p.i.

Supplemental Figure 2 Detection and kinetics of AMA-1–specific B cells after *P. yoelii* infection. Representative flow plot showing gated AMA-1–specific B cells from naïve and day 70 infected C57BL/6 mice identified after excluding dead, doublets, and non-B cells ($CD3^+CD11b^+Ter119^+$) and enrichment with MSP-1 and decoy tetramers. (B) Total number of AMA-1^+ B cells over 467 days p.i. (C) Representative gating strategy used to identify AMA-1^+ isotype switched and IgM^+ MBCs based on CD73 and CD80 staining at day 56 p.i. Total number

of AMA-1^{+} swIg^{+} or IgM^{+} (D) CD73^{+}CD80^{+} or (E) CD73^{-}CD80^{-} MBCs over 467 days p.i. Each data point shows the mean ± S.E.M. with 3-5 mice per time point from two independent experiments.

Supplemental Figure 3 Expression of IgD on different MBC populations after *P. yoelii* infection. Representative flow plots showing the gates used to distinguish IgD^{hi} and IgD$^{lo/-}$ B cells within the MSP-1–specific IgM^{+} and swIg^{+} CD73^{+}CD80^{+} and CD73^{-}CD80^{-} MBC pools at day 90 p.i. The graph displays the frequency of IgD^{hi} B cells amongst the MSP-1–specific MBC populations at day 90 p.i. Each data point shows the mean ± S.E.M. with n = 3 mice. Data are representative of two independent experiments.

Supplemental Figure 4 swIg^{+} CD80^{-}CD73^{-} B cells fail to expand and upregulate ZsGreen1 expression after adoptive transfer and challenge with *P. yoelii*. (A) Representative flow plots showing the gating strategy to identify ZsGreen1^{+} cells derived from donor cells at day 8 p.i. (B) Representative flow plots showing the gating strategy to identify CD45.2^{+} cells derived from donor cells at day 8 p.i. (C) Total number of recovered donor cells at day 8 p.i. (D) Representative flow plots showing the gating strategy to identify ZsGreen1^{+} cells derived from donor cells at day 28 p.i. (E) Representative flow plots showing the gating strategy to identify CD19^{+}CD45.2^{+} B cells derived from donor cells at day 28 p.i. (F) Total number of recovered donor cells at day 28 p.i. (C, E) Each data point shows the mean ± S.E.M. with 2-6 mice per time point from two independent experiments. Significance was calculated by one-way ANOVA Kruskal-Wallis test with post hoc Dunn's multiple comparisons test. *$p < 0.05$.

Figure 1

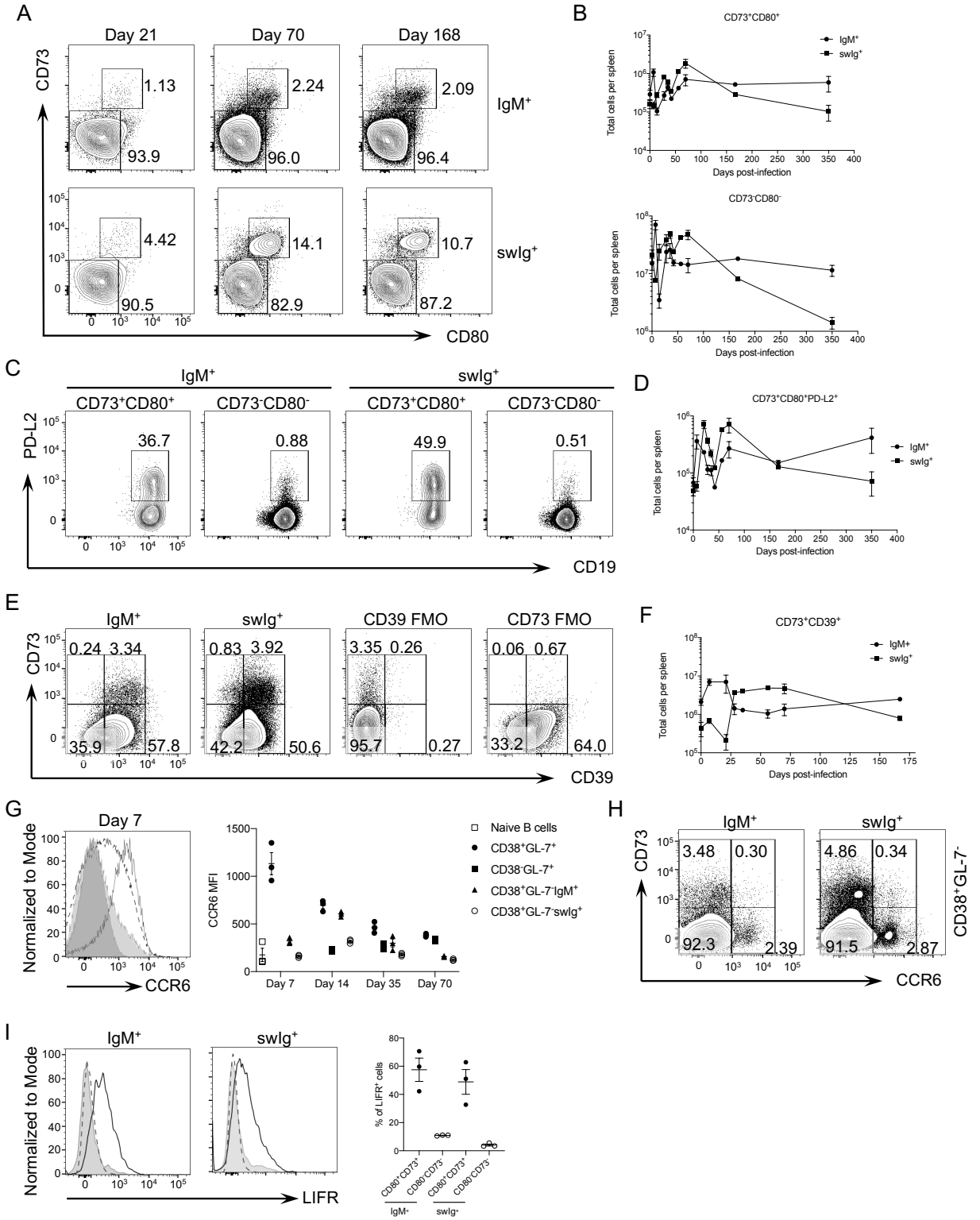
A
Day 21
Day 70
Day 168
CD73
CD80
IgM+
swIg+
1.13
93.9
2.24
96.0
2.09
96.4
4.42
90.5
14.1
82.9
10.7
87.2
B
CD73+CD80+
CD73-CD80-
Total cells per spleen
Days post-infection
IgM+
swIg+
C
IgM+
swIg+
CD73+CD80+
CD73-CD80-
PD-L2
CD19
36.7
0.88
49.9
0.51
D
CD73+CD80+PD-L2+
E
IgM+
swIg+
CD39 FMO
CD73 FMO
CD73
CD39
0.24 3.34
35.9 57.8
0.83 3.92
42.2 50.6
3.35 0.26
95.7 0.27
0.06 0.67
33.2 64.0
F
CD73+CD39+
G
Day 7
Normalized to Mode
CCR6
CCR6 MFI
Naive B cells
CD38+GL-7+
CD38-GL-7+
CD38+GL-7-IgM+
CD38+GL-7-swIg+
Day 7
Day 14
Day 35
Day 70
H
IgM+
swIg+
CD73
CD38+GL-7-
CCR6
3.48 0.30
92.3 2.39
4.86 0.34
91.5 2.87
I
IgM+
swIg+
Normalized to Mode
LIFR
% of LIFR+ cells
CD80+CD73+
CD80-CD73-
CD80+CD73+
CD80-CD73-
IgM+
swIg+

Figure 2

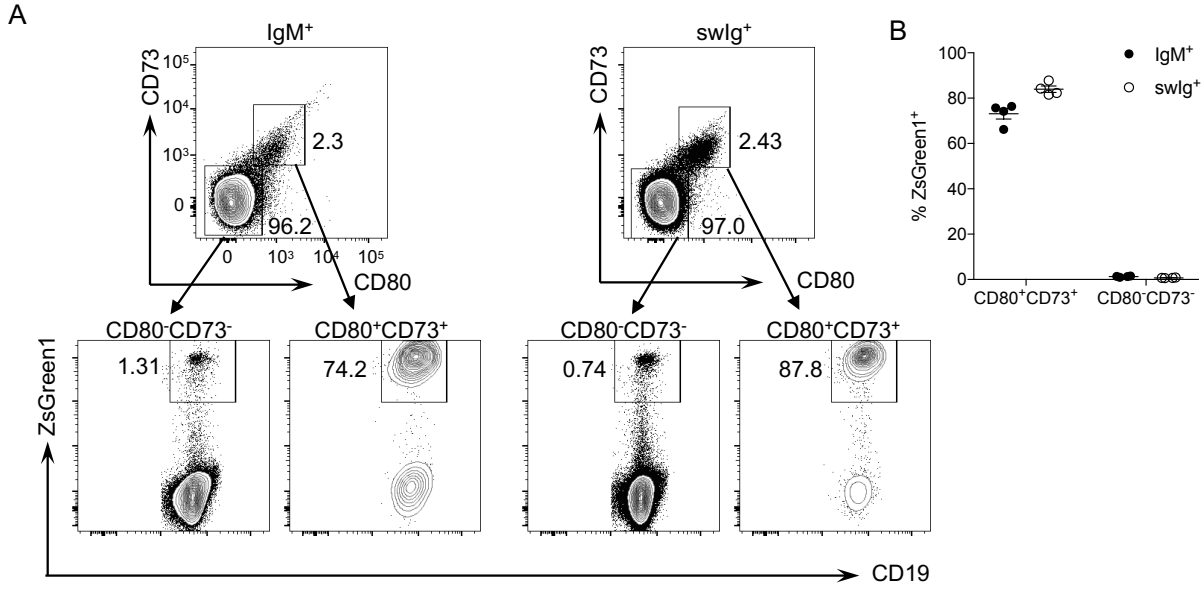
A
IgM+
CD73
CD80
2.3
96.2
swIg+
2.43
97.0
CD80-CD73-
CD80+CD73+
1.31
74.2
0.74
87.8
ZsGreen1
CD19
B
IgM+
swIg+
% ZsGreen1+
CD80+CD73+
CD80-CD73-

Figure 3

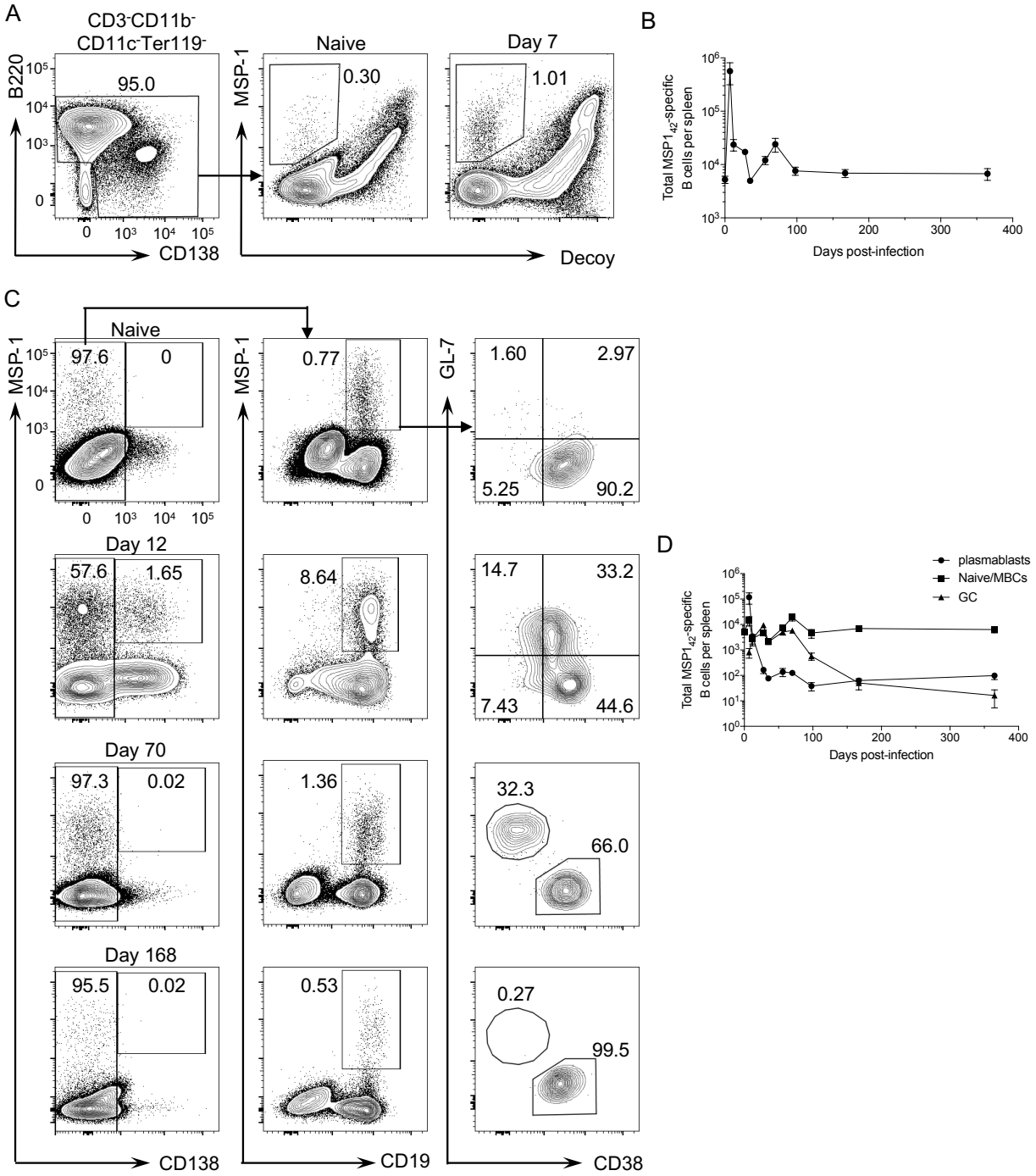
A
CD3-CD11b-
CD11c-Ter119-
B220
95.0
CD138
Naive
MSP-1
0.30
Day 7
1.01
Decoy
B
Total MSP142-specific
B cells per spleen
Days post-infection
C
Naive
97.6
0
0.77
1.60
2.97
5.25
90.2
Day 12
57.6
1.65
8.64
14.7
33.2
7.43
44.6
Day 70
97.3
0.02
1.36
32.3
66.0
Day 168
95.5
0.02
0.53
0.27
99.5
GL-7
CD19
CD38
D
plasmablasts
Naive/MBCs
GC

Figure 4

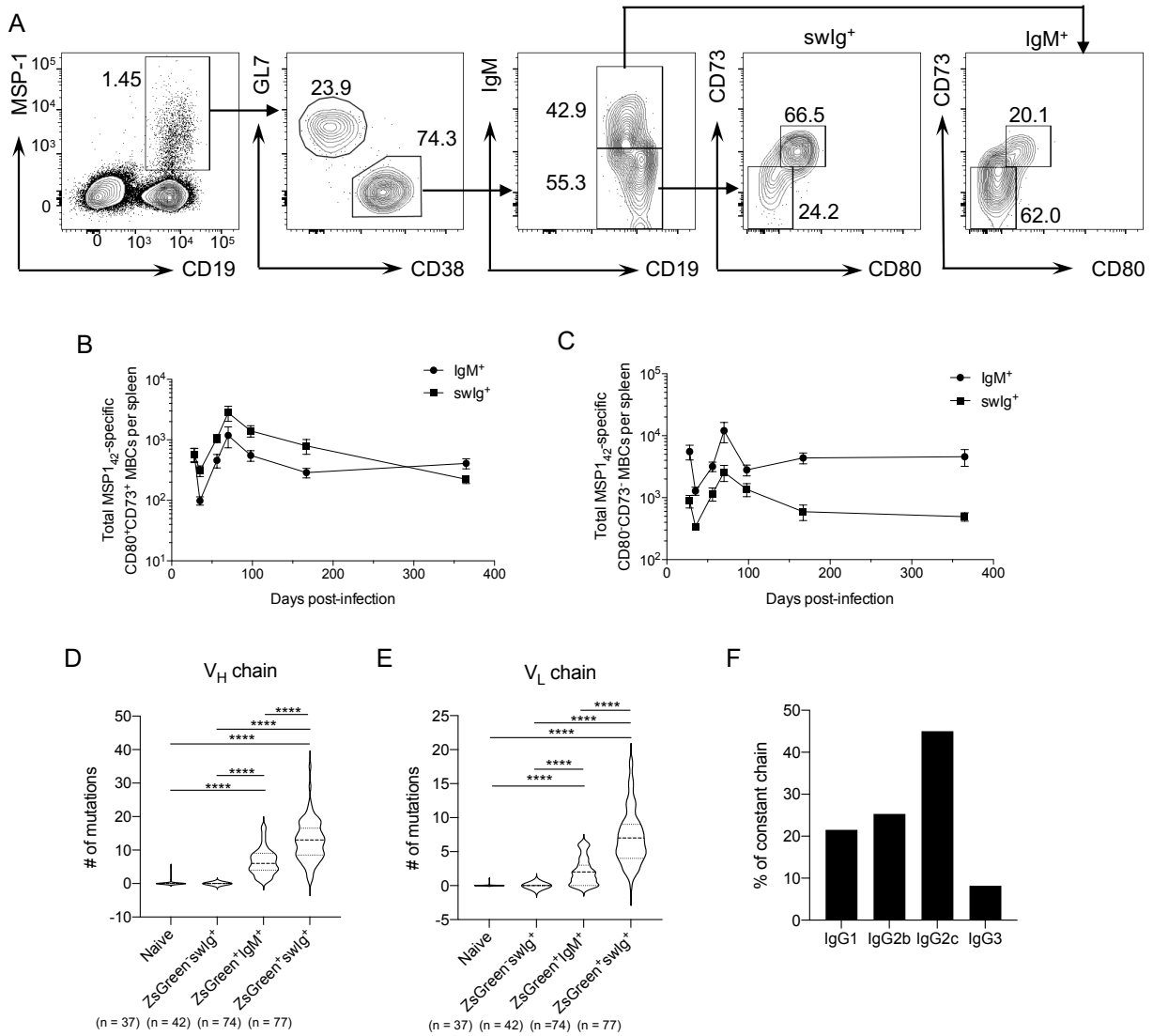
A
MSP-1
1.45
CD19
GL7
23.9
74.3
CD38
IgM
42.9
55.3
CD19
CD73
swIg+
66.5
24.2
CD80
CD73
IgM+
20.1
62.0
CD80
B
IgM+
swIg+
Total MSP1 42-specific CD80+CD73+ MBCs per spleen
Days post-infection
C
IgM+
swIg+
Total MSP1 42-specific CD80-CD73- MBCs per spleen
Days post-infection
D
VH chain
# of mutations
Naive
ZsGreen-swIg+
ZsGreen+IgM+
ZsGreen+swIg+
(n = 37) (n = 42) (n = 74) (n = 77)
E
VL chain
# of mutations
Naive
ZsGreen-swIg+
ZsGreen+IgM+
ZsGreen+swIg+
(n = 37) (n = 42) (n =74) (n = 77)
F
% of constant chain
IgG1
IgG2b
IgG2c
IgG3

Figure 5

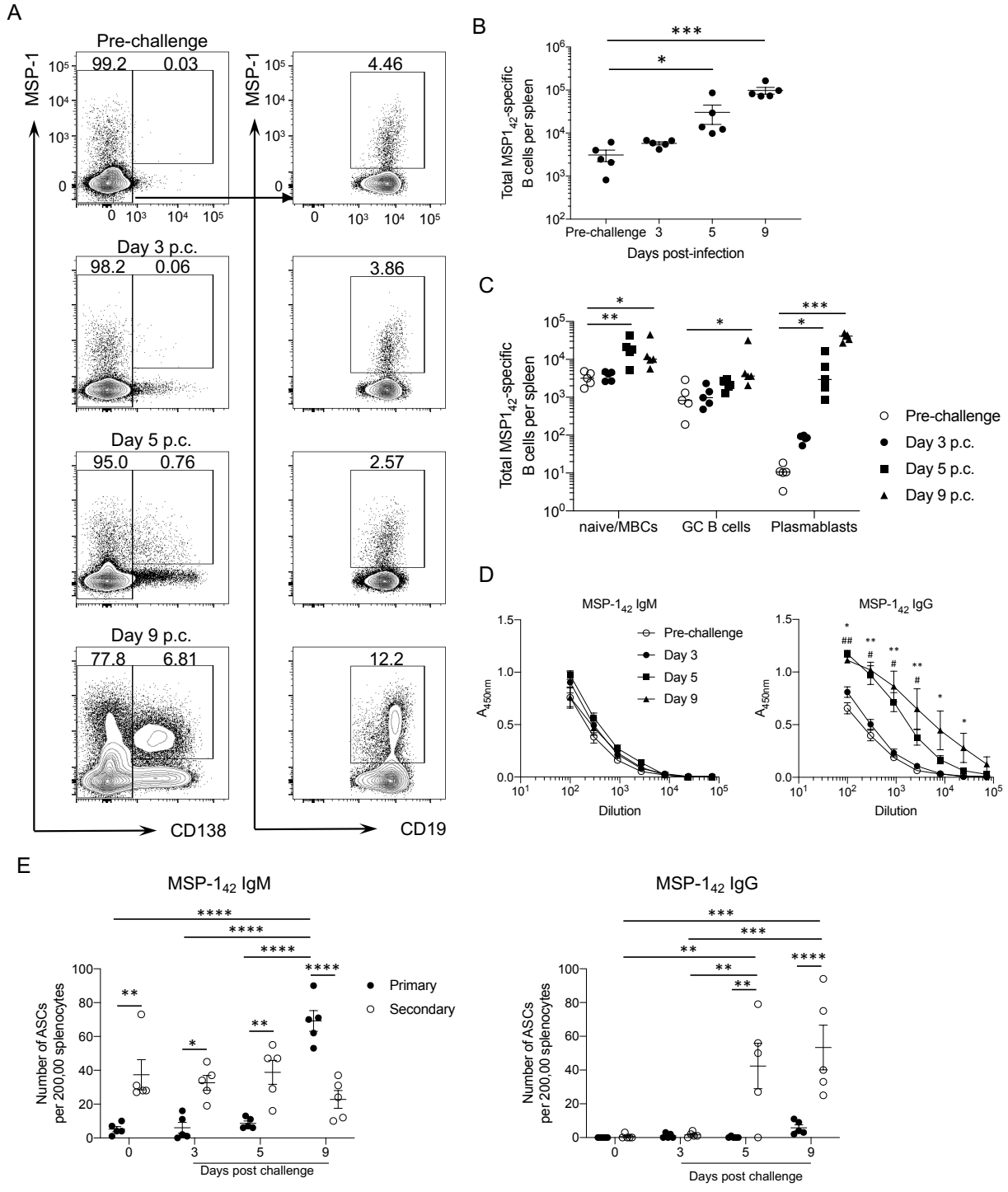
A
Pre-challenge
99.2
0.03
4.46
Day 3 p.c.
98.2
0.06
3.86
Day 5 p.c.
95.0
0.76
2.57
Day 9 p.c.
77.8
6.81
12.2
MSP-1
CD138
CD19
B
Total MSP1$_{42}$-specific B cells per spleen
Days post-infection
Pre-challenge
C
naive/MBCs
GC B cells
Plasmablasts
Pre-challenge
Day 3 p.c.
Day 5 p.c.
Day 9 p.c.
D
MSP-1$_{42}$ IgM
MSP-1$_{42}$ IgG
A_{450nm}
Dilution
E
Number of ASCs per 200,00 splenocytes
Days post challenge
Primary
Secondary

Figure 6

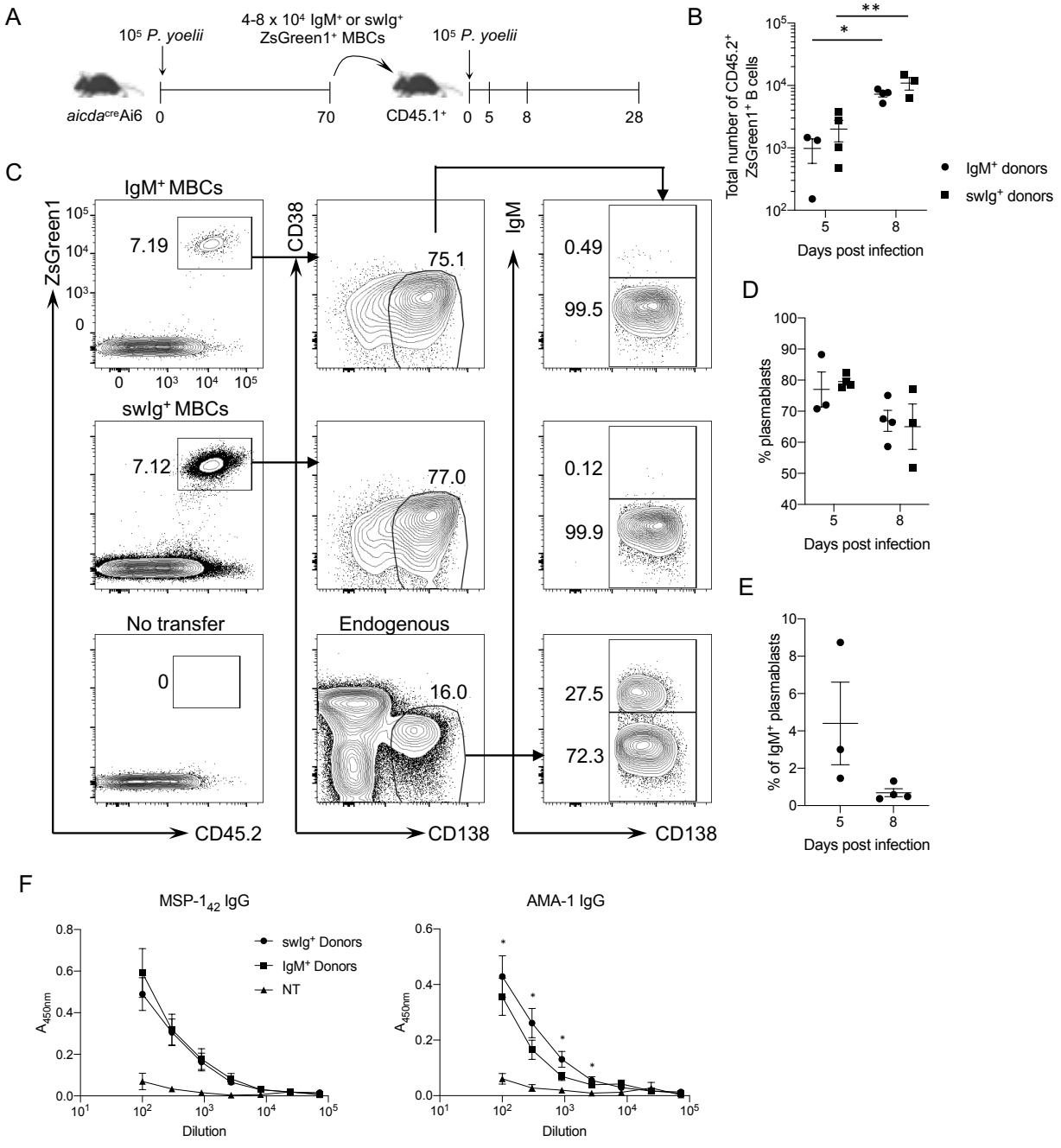
A
10⁵ P. yoelii
4-8 x 10⁴ IgM⁺ or swIg⁺ ZsGreen1⁺ MBCs
10⁵ P. yoelii
aicdacreAi6
0
70
CD45.1⁺
0 5 8
28
B
Total number of CD45.2⁺ ZsGreen1⁺ B cells
Days post infection
IgM⁺ donors
swIg⁺ donors
C
IgM⁺ MBCs
swIg⁺ MBCs
No transfer
Endogenous
ZsGreen1
CD38
IgM
7.19
75.1
0.49
99.5
7.12
77.0
0.12
99.9
0
16.0
27.5
72.3
CD45.2
CD138
CD138
D
% plasmablasts
Days post infection
E
% of IgM⁺ plasmablasts
Days post infection
F
MSP-1₄₂ IgG
AMA-1 IgG
swIg⁺ Donors
IgM⁺ Donors
NT
A450nm
Dilution

Figure 7

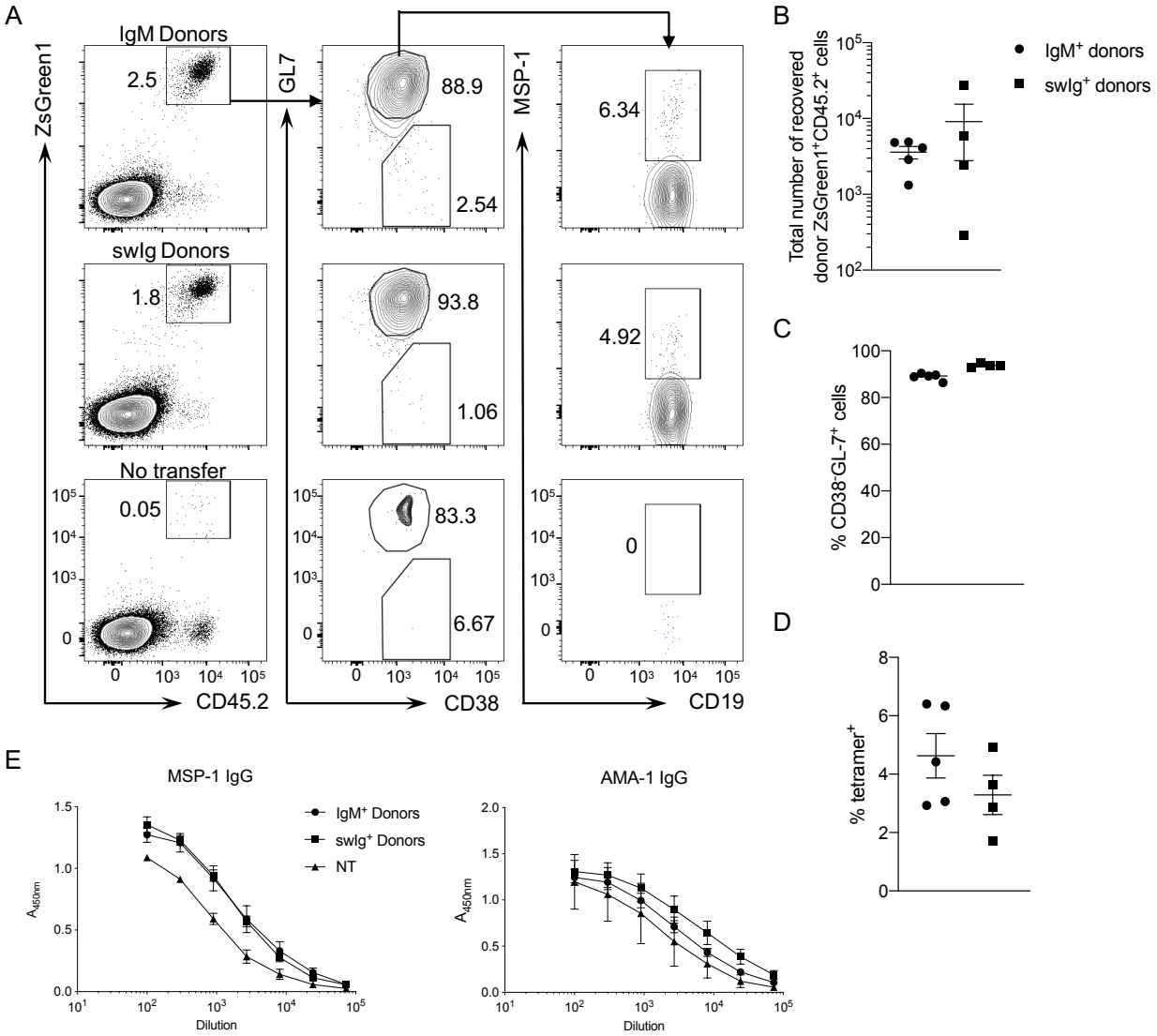
A
IgM Donors
swIg Donors
No transfer
ZsGreen1
GL7
MSP-1
CD45.2
CD38
CD19
2.5
88.9
2.54
6.34
1.8
93.8
1.06
4.92
0.05
83.3
6.67
0
B
Total number of recovered donor ZsGreen1+CD45.2+ cells
IgM+ donors
swIg+ donors
C
% CD38-GL-7+ cells
D
% tetramer+
E
MSP-1 IgG
AMA-1 IgG
IgM+ Donors
swIg+ Donors
NT
A450nm
Dilution

Figure 8

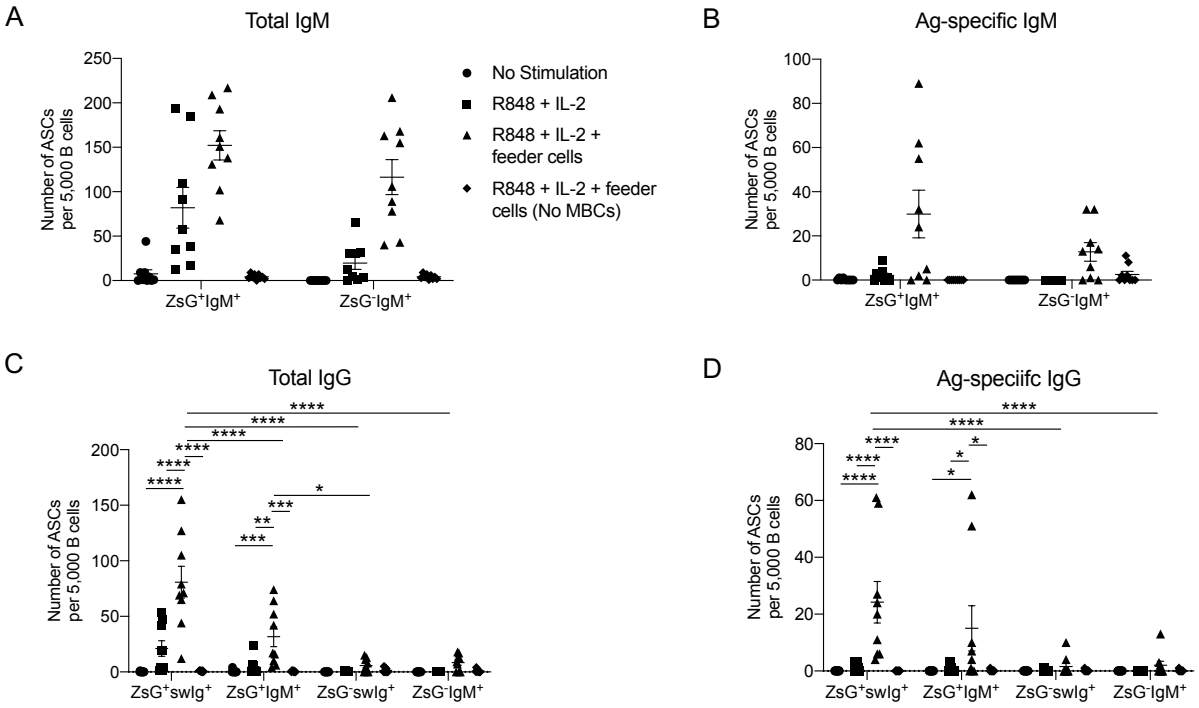
A
Total IgM
Number of ASCs per 5,000 B cells
250
200
150
100
50
0
ZsG+IgM+
ZsG-IgM+
No Stimulation
R848 + IL-2
R848 + IL-2 + feeder cells
R848 + IL-2 + feeder cells (No MBCs)
B
Ag-specific IgM
Number of ASCs per 5,000 B cells
100
80
60
40
20
0
ZsG+IgM+
ZsG-IgM+
C
Total IgG
Number of ASCs per 5,000 B cells
200
150
100
50
0
****
****
****
****
****
****
*
***
**
***
ZsG+swIg+
ZsG+IgM+
ZsG-swIg+
ZsG-IgM+
D
Ag-speciifc IgG
Number of ASCs per 5,000 B cells
80
60
40
20
0
****
****
****
****
****
*
*
*
ZsG+swIg+
ZsG+IgM+
ZsG-swIg+
ZsG-IgM+

Supplemental Figure 1

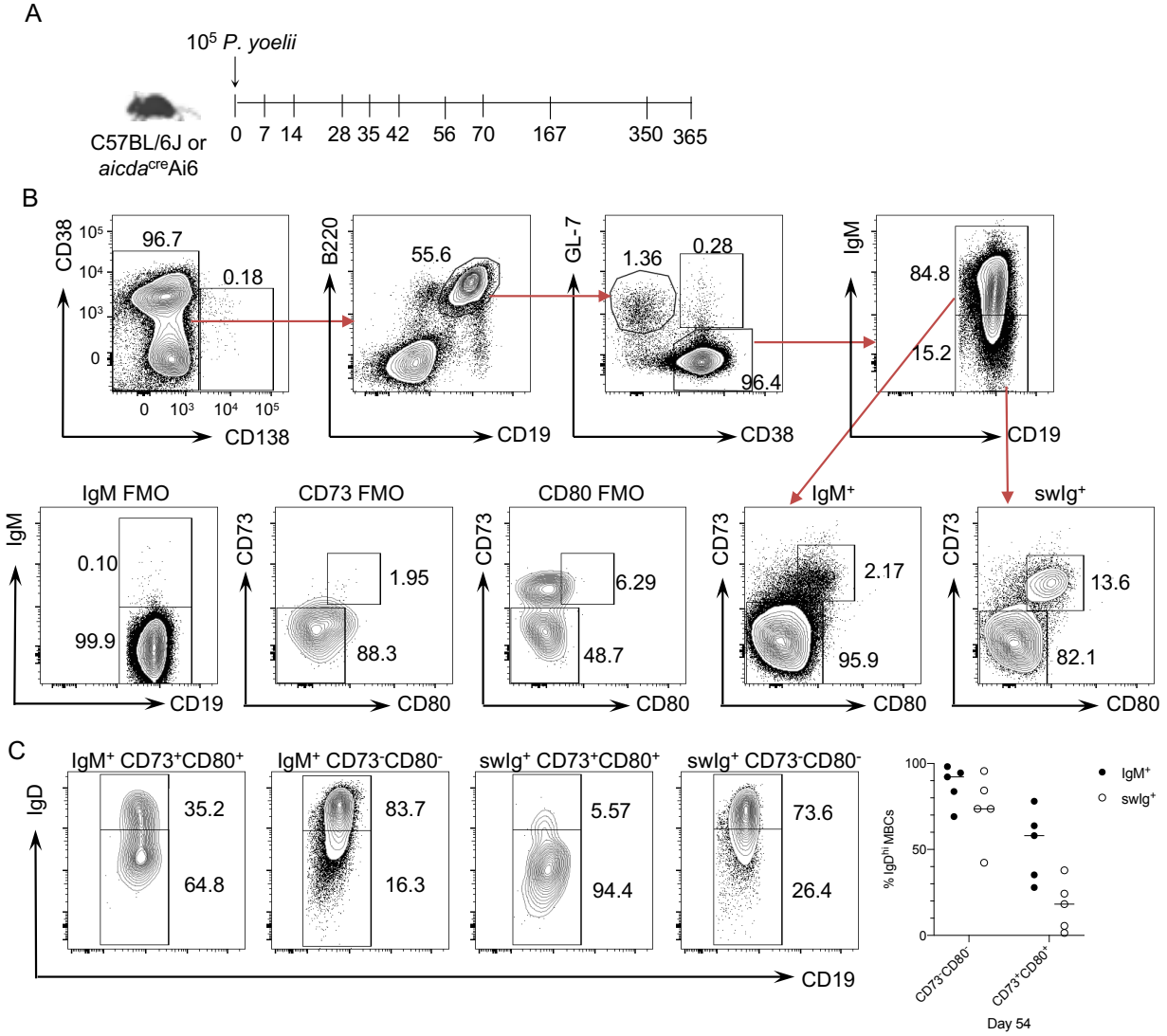

Supplemental Figure 2

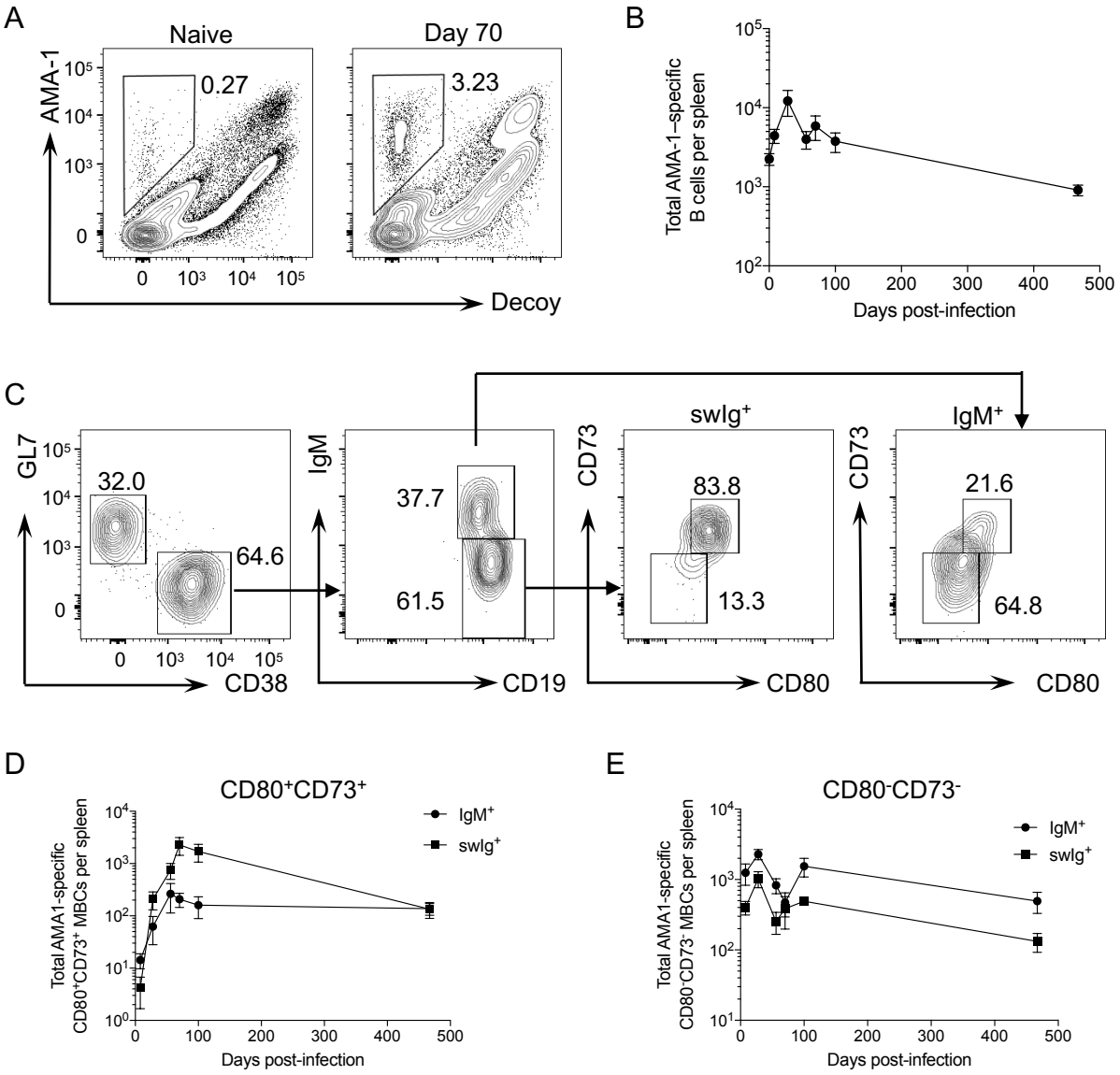

Supplemental Figure 3

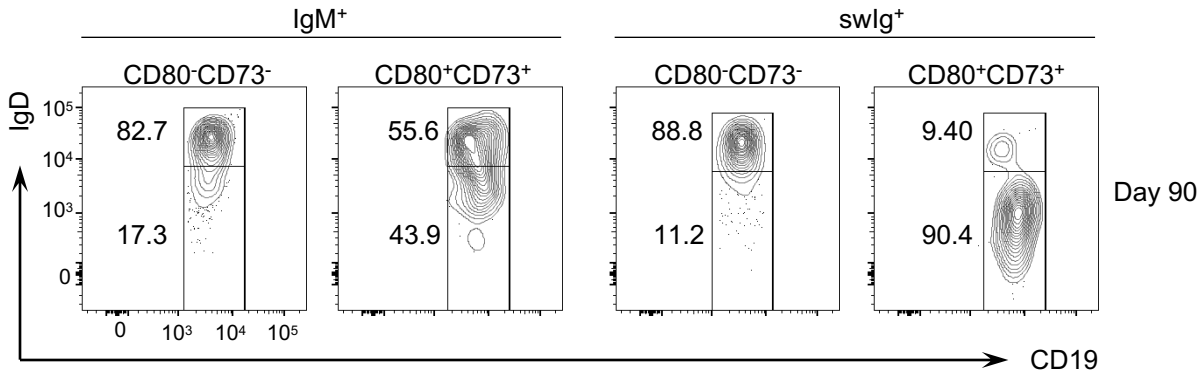

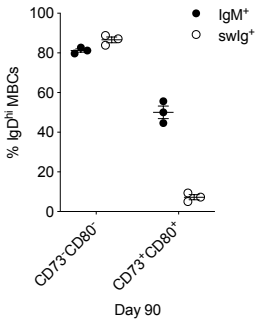
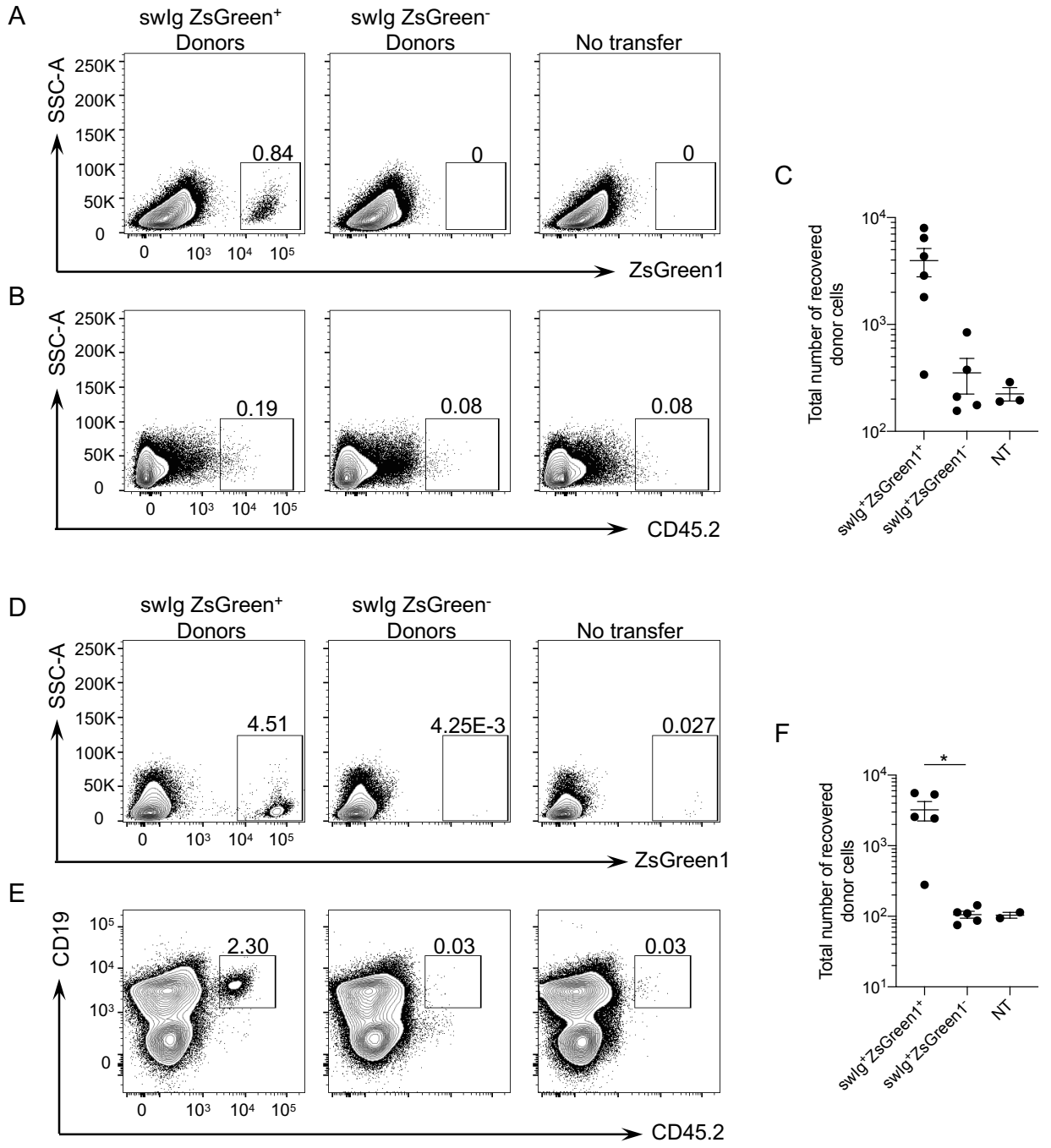
Supplemental Figure 4